Ref: NHESS-2017-41

Dear Editor,

First of all, we warmly thank you for constructive comments. We followed your suggestions to revise the manuscript.

Regarding the two main points you highlighted:

- *the difference of your compilation with respect to DISS database (first point in Main Comments by RC1; L50-51 in Section Specific Comments by RC2).*
  We improved the manuscript (lines 123-149), giving an explanation of our choice about the fault database. In particular, we analysed the individual sources included in the DISS and spotted some issues that include: (i) the lack of updating of the geological information of some individual sources and (ii) the nonconformity between the input data used by DISS in Boxer and the latest historical seismicity (CPTI15) and macroseismic intensity (DBMI15) publications.
  Thus, we preferred to performed a full review of the fault database, compiling a fault source database as a synthesis of works published over the past twenty years, using all updated and available geological, paleoseismological and seismological data (see the supplemental files for a complete list of references).

- *the rationale and consequences of using end-member MFD models (L402 on by RC1;L207:211 by RC2).*
  We explained this in the introduction at L64-83. As we know, the choice of the "appropriate" MFD for each fault source is a difficult task because palaeoseismological studies are scarce, and it is often difficult to establish clear relationships between mapped faults and historical seismicity. Today, the discussion is still open and far from being solved with the available observations, including both seismological and/or geological/paleoseismological observations. What we did in this work, was to adopt two widely-used MFDs, a characteristic Gaussian model and a Truncated Gutenberg-Richter model, to explore the epistemic uncertainties. Finally, we considered also a Mixed model as a so-called "expert judgement" model. Obviously, this approach does not solve the issue, and the choice of MFD remains an open question in fault-based PSHA

Moreover, we used the last update version of the CPTI15, so some figures have been updated (Fig. 4,5,9,11,12 and 13).

Finally, the manuscript has been edited by mother-tongue American Journal Experts (AJE, www.aje.com) for proper English grammar and style.

Sincerely,

Alessandro Valentini

(Corresponding author)

Review of manuscript NHESS-2017-41 "Integrating faults and past earthquakes into a probabilistic seismic hazard model for peninsular Italy" by Alessandro Valentini, Francesco Visini & Bruno Pace

Main comments

This manuscript describes an approach to model seismic hazard in Italy using a combination of active fault data and gridded seismicity based on the instrumental and historical earthquake catalog. A database of active faults has been compiled, and important historical earthquakes have been assigned to their causative faults. Two models are considered for the magnitude-frequency distributions (MFDs) of the faults, either a truncated Gutenberg-Richter (TGR) MFD or a characteristic Gaussian (CHG) MFD. The gridded source model accounts for off-fault seismicity, and its MFD is computed in a way that it is complementary to the MFD of the fault source model (using a threshold magnitude, avoiding double-counting of earthquakes assigned to faults, and an additional weighting function that reduces gridded seismicity in the vicinity of faults). The authors explore the impact of the two MFD models, as well as the contribution of fault sources and gridded seismicity to the total hazard. They also define a preferred source model, in which the most appropriate MFD model for each fault is selected.

The approach to model fault sources is state of the art, and the integration of fault sources and gridded seismicity contains some innovative elements. The manuscript is mostly well written (with some exceptions, which are pointed out in the detailed comments below), the figures are clear, and the references are appropriate. The conclusions are supported by the results.

However, a number of improvements need to be made before the manuscript can be published. Below, I have listed a number of detailed comments. I summarize my main comments here:

- A major shortcoming is that the paper does not contain any reference to other published fault source models for Italy, notably DISS (Database of Individual Seismogenic Sources, http://diss.rm.ingv.it/diss/). At the very least, the authors should indicate how their fault source model relates to DISS, and what are the main differences (concepts and/or data).

- *We will add these information in the section 2.1 "Fault Source Model" at line 84: "Although for the Italian territory there is already a database that contains the results of the investigations of the active tectonics during the past 20 years (Database of Individual Seismogenic Sources, DISS, http://diss.rm.ingv.it/diss/), made by three main categories of seismogenic sources: individual seismogenic sources, seismogenic areas, macroseismic sources, it does not work well to elaborate a PSHA model using individual seismogenic sources, as in this work. In* *fact, the DISS Authors (Basili et al., 2008) say that the individual seismogenic sources database cannot guarantee the completeness of the sources themselves and are not meant to comprise a complete input dataset for probabilistic assessment of seismic hazard. For this reason, we are not restricted to just use of the DISS, but trough a synthesis of published works over the last twenty years (see supplements for complete references) we defined a database as complete as possible, in terms of individual seismogenic sources, and parameters to have input dataset for PSHA."*

- Although the authors refer to the SHARE project, and even use certain aspects of it, they do not compare their results to the fault-based hazard map (FSBG model) created in this project.
- Similarly, although a comparison with the current national hazard map is described in general terms, this comparison is not shown.

- *We attach in supplement a figure (Figure S1) showing the comparison among SHARE (FSBG) model, the current Italian national seismic hazard map (MPS04) and our model (Mixed model), using the same GMPE's. The new figure we'll be included in the manuscript, at Chapter 3. The figure shows how the impact of our fault sources input is more evident then the FSBG-Share model (the branch using fault sources and background) and the comparison with MPS04 confirm a similar pattern, but with some significant differences at the regional-to-local scale.*

- In my opinion, it is also essential to show the summed MFDs of the different source models, and comparing those to each other and to the observed MFD based on the full catalog. Without this information, it is not possible to evaluate the performance of their model. Notably, it is indicated that the rate of M 5.5-6.0 earthquakes in the TGR end member is higher than in the CHG end member, but this is not shown.

- *Thanks for your suggestion. We attach in supplement a figure (Figure S2) showing and comparing the summed MFD's of the fault source inputs (TGR, CHG, Mixed), the distributed source input, the total model (distributed + fault) and the CPTI15 catalogue, for Apennines and surrounding areas. This new figure highlights also the differences in the rate of M 5.5-6.0 earthquakes between TGR and CHG model. The new figure we'll be included in the revised version of the manuscript.*

- I have some doubt whether maximum magnitudes are correctly modelled, as it is indicated at some point that an earthquake assigned to a fault could have a magnitude larger than the magnitude range in the MFD for that fault, which should not be allowed.

- *What we wrote at lines 442-444 was a mistake: we never have a magnitude larger than the magnitude range in the MFD for a fault. So, the right sentence is: "if an earthquake* *assigned to a fault source (see Table 2 for earthquake-source associations) has a magnitude lower than the magnitude range in the bell curve of the CHG model distribution, the TGR model is applied to that fault source." We'll update the text in the revised version of the manuscript.*

- To improve clarity, the authors should more clearly explain in advance what they intend to do. Two main cases are:

  - They first describe the fault-source model and the distributed source model, and only later explain that these are not independent models, but are complementary, together accounting for all seismicity in Italy;

  - *You are right, we'll write in the revised version of the manuscript, as you suggest, that the two models are not independent but complementary, both in magnitude and frequency distribution. Moreover, as also suggested by the second reviewer, the fault-source and distribute source are not 'models' s.s., so we'll rename them as 'input'.*

  - They first show hazard maps produced with the TGR and CHG MFD models, but only later explain that these are two end members, and that their preferred model is the Mixed model, in which a particular MFD model is assigned to each fault.

  - *Thanks for your suggestion. We'll be more clear in the introduction of the revised version of the manuscript that we consider the TGR and CHG MFD models as end members, and the Mixed model as a sort of an "expert judgment" model, useful for comparison analysis.*

Detailed comments

Abstract

L. 30: "the spatial pattern of our model is far more detailed" → "the spatial pattern of the hazard maps obtained with our model is far more detailed". Unfortunately, this is not demonstrated in the paper, as there is no direct comparison with other hazard maps.

We'll show the differences between our approach and the others by a figure (Figure S1 in the supplement) where we compare our results with SHARE (FSBG) model and the current national hazard map (MPS04), using the same GMPE's. The new figure we'll be included in the manuscript, at Chapter 3.

1. Introduction

L. 52: “Combining seismic hazards from active faults with background sources” → “Combining active faults with background sources”. I also note that the plural “seismic hazards” is used in other places in the manuscript, but it should be singular, as the paper deals with only one type of seismic hazard, namely ground-motion seismic hazard.

Thanks for your suggestion: we’ll remove the plural.

2.1 Fault Source Model

L. 92: “thrust faults could be considered in a future study”: Is there a particular reason for not including thrust faults in the present study? And for which areas in Italy will this have the largest impact?

We decided to not include thrust faults in the present study because for them we have to solve some problems, mainly connected to the definition of individual seismogenic source, not yet solved in Italy for such kind of structure. For example, for thrust faults we do not have a good knowledge of the geological slip rate as for normal active fault, we need to introduce a different way to make the segmentation and different segmentation rules, and maybe there is need to consider them as complex sources in OpenQuake. The areas in Italy where we think they will have the largest impact are NE sector of the Alps, Po Valley, offshore sector of the central Adriatic Sea and SW Sicily. In this paper we want to focus on the impact of the integration of faults and earthquakes data, without the assumption to be complete in terms of individual seismogenic source database, but on the contrary suggesting a way to integrate two incomplete database in the best way, without throwing data. We will add in the manuscript a phrase explaining our choices.

L. 101-102: “Slip rates control fault-based seismic hazards … and provide a time scale …”: Strange phrasing. Slip rates do not provide a time scale. I’m not sure whether the authors mean to say that slip rates may be measured over different time scales or that slip rates may vary through time or both.

Thanks for your suggestion: we will rephrase this sentence as: “Slip rates control fault-based seismic hazard … and reflect the velocity of the mechanisms operating during continental deformation ...”

L. 112-124: This paragraph discusses slip rate variability through time, and states that slip rates have been determined for different time scales. However, (1) it is not clear how this time variability is handled in this study (it is not mentioned anymore further in the paper), and (2) Table 1 only lists minimum and maximum slip rates, without indication of the corresponding time scale. Is the time scale the same for all faults in this table?

Thanks for your suggestion: this paragraph is not clear and so we will re-write it in the revised version of the manuscript. The aim is to highlight that we are conscious of the problem of the possible slip term variability through time, but we are able to solve it with the data in our database. The assumption we do is that we use the minimum and maximum values of slip rate, determined in different ways and different time scales (see the numerous neotectonics, palaeseismological and seismotectonics cited papers), to calculate a mean value that we assume as representative of the long term behaviour (about last 15 ka for the Apennines).

L. 141: "the function with the lowest log-likelihood": Shouldn't this be the highest log-likelihood? Usually, one seeks the maximum likelihood, not the minimum likelihood

Yes, it is the highest log-likelihood. We'll correct in the revised version of the manuscript.

L. 145-150: Is this an appropriate way to determine the overall standard deviation of the slip rate distribution in an area? I think it would be more appropriate to apply the Central Limit Theorem. If you consider each fault slip rate (x) as a sample from a population with mean μ and standard deviation σ, then μ can be found as μ_x(mean value of the sample means), and σ as $\sqrt{n}\,\sigma_x$ (with n the number of samples and the standard deviation <u>of the sample means</u>).

Thanks for this suggestion. We applied the Central Limit Theorem for the three areas and the standard deviation is 0.11, 0.33 and 0.83 for Northern, Central-Southern, and Calabria-Sicilian area respectively. Instead using our approach we obtained 0.25, 0.29, and 0.35 for the three areas respectively. The obtained values for Northern and Calabrian-Sicilian areas are a little bit different, we think because the sample population is not enough large to apply the Central Limit Theorem; in fact n has to be > 30, while in our case n is equals 20 and 14 for the Northern and Calabrian-Sicilian area respectively. For this reason we decided to leave the standard deviation computed with our suggested approach.

L. 166-169: there seems to be overlap between criterion ii (sharp bends) and criterion iv (bending ≥ 60°).

Yes, you are right, we wrote in a wrong way. The ii criterion is "(ii) intersections with cross structures (often transfer faults) extending 4 km along strike….". We will correct the manuscript.

L. 180: "thinnest ST" → "smallest ST". Can you comment on the small ST value of 2.5 km? Is this in a volcanic zone?

No, it is not in a volcanic zone. The value of 2.5 km is due to the presence of "Alto Tiberina Fault". It is a structure well known in literature: a low angle normal fault acts to detachment *for the seismogenic faults located in the hanging-wall. We'll add a sentence in the revised manuscript at line 180 as: "with the thinnest ST is Monte Santa Maria Tiberina (id 9, ST = 2.5 km) due to the presence of east-dipping low angle normal fault, the Alto-Tiberina Fault (Boncio et al., 2000), located few kilometres west of the is Monte Santa Maria Tiberina fault."*

L. 181: "Observed maximum magnitude data have been assigned to 47 fault sources". Is this based on Table 2?

Yes, it is. We have written it in the manuscript at line 181:" Observed maximum magnitude data have been assigned to 47 fault sources (based on Table 2)".

L. 197-198: "a value that corresponds to the maximum observed magnitude (Mobs)". I'm not convinced it is correct to consider Mobs as one of the possible Mmax values, and treat it the same as the other estimations. In fact, the only thing we know for sure about Mmax is that it cannot be lower than Mobs. For that reason, Mobs is often used as a lower truncation of Mmax distributions (e.g.,EPRI method for Stable Continental Regions). Not doing this can have strange consequences, as in lines 442-444, where it is stated "If an earthquake assigned to a fault source has a magnitude lower or higher than the bell curve of the CHG model distribution, …". However, the second case (observed magnitude higher than modelled Mmax distribution) should not be allowed in the PSHA model.

We partially agree with you. In some cases the observed Magnitude (Mobs) is useful to better constrain the potentiality of an individual seismogenic source, as some examples like Irpinia Fault (id 51 in the database) where the 1980 earthquake helps to better constrain the Mmax computed by only scaling relationships. Obviously it is important to avoid cases where there is an inconsistency between the fault geometry and the observed magnitude, and so our rationale was:

1) *we calculate the maximum expected magnitude (Mmax1), and the relative uncertainties, using only the scaling relationships (detail in Pace et al., 2016, FiSH paper);*
2) *we compared the observed magnitude of the associated earthquakes in the catalogue (Mobs), and if the Mobs is contained in the range Mmax1 +-1 standard deviation, we consider the Mobs recalculating the Mmax (Mmax2) and the new uncertainties;*
3) *if the Mobs is lower then Mmax1 we consider a GR behaviour for the source, without using the Mobs in the Mmax2 calculation;*
4) *if the Mobs is larger then Mmax1 we review the fault geometry or the earthquake source association.*

We'll improve the manuscript in order to better explain our rationale.

L. 199: "modifying the along-strike dimension if the rupture length exceeds the length predicted by the aspect ratio relationships". This is not very clear. Maybe rephrase as "reducing the fault length if the aspect ratio (W/L) is smaller than indicated by the relation between aspect ratio and rupture length for observed earthquake ruptures in the Abruzzo (Peruzza & Pace, 2002)".

Thanks for this suggestion. We'll rephrase as you suggest.

L. 202: "we use the criterion of "segment seismic moment conservation"": is this a criterion or a concept, and can you briefly describe what it implies?

We agree that a brief description could be useful. At line 203 we'll add a sentence as: "… which divides the seismic moment that corresponds to M_{max} by the moment rate given a slip rate:

$$T_{mean} = \frac{1}{Char\_Rate} = \frac{10^{1.5M_{max}9.1}}{\mu VLW}$$

where T_{mean} is the mean recurrence time in years, Char_Rate is the annual mean rate of occurrence, M_{max} is the computed mean maximum magnitude, μ is the shear modulus, V is the average long-term slip rate, and L and W are the geometrical parameters of the fault, along-strike rupture length and down dip width respectively."

L. 206-207: "we use two magnitude-frequency distributions" → "we use two magnitude-frequency distribution models". I also recommend introducing the acronym MFD here, as the term is used frequently in the remainder of the manuscript.

Thanks for the suggestion: we'll introduce the acronym MFD in the abstract and replaced all "magnitude-frequency distribution" in the manuscript.

L. 208: "Gaussian bell curve centred on the Mmax": Perhaps it is worth mentioning that this Gaussian curve applies to the incremental MFD values, not to the cumulative MFD values that are shown in Fig. 2c.

We'll modify the sentence into: "symmetric Gaussian bell curve (applied to the incremental MFD values) centred on the Mmax of each fault, with a range of magnitudes equal to 1-sigma".

L. 209-211: It is not explained how the a- and b-values are determined for each fault when the TGR model is used. I assume this is done with the FiSH code, but it would be good to briefly describe the underlying concept (relation with slip rate).

We'll add a phrase to better explain how the a- and b-values have been determined: "For MFD, the b-value is constant and equal to 1.0 for all faults, obtained by the interpolation of the earthquakes in the CPTI15 catalogue, as the events on the single sources are *insufficient for statistics. However the a-values have been computed by Activity Rate FiSH code, balancing the total expected seismic moment rate with the seismic moment rate that was obtained by the pair M_{max} and T_{mean}, evaluated by the fault geometry and the slip rate of each individual source (details in Pace et al., 2016)."*

2.2 Distributed Source Model

L. 233-234: "If the causative source of an earthquake is known, the impact of that earthquake does not need to be included in the seismicity smoothing process" → "If the causative fault of an earthquake is known, that earthquake does not need to be included in the seismicity smoothing procedure". It should be explicitly mentioned before that the fault and distributed source models are conceived as complementary source models, not as alternative source models (competing models in a logic tree). In the latter case, they should be independent.

Thanks for this suggestion. We'll better explain before that we consider the two source models complementary but not alternative, and so not independent.

L. 263: I think the * symbol in the equation should be left out. If I understand correctly, rather than a multiplication, $\lambda(i_x, i_y)$ represents the seismicity rate in grid cell (i_x,i_y)

Yes, you are right, it was a typo.

L. 276-278: I don't understand the description of the Voronoi partition procedure: if the Italian territory is divided in a grid with 0.05° lon/lat spacing, then how can the number of grid cell centres be varied? Perhaps the centres of the grid cells represent the possible centres of Voronoi polygons, and you vary the number of Voronoi polygons from 3 to 50, for each case drawing 1000 random subsets of Nv grid cell centres?

To be more clear we'll modify the manuscript as:"… the Voronoi tessellation of space without tectonic dependency. The whole Italian territory has been divided into a grid with a longitude/latitude spacing of 0.05°, and the centres of the grid cells represent the possible centres of Voronoi polygons. We vary the number Voronoy poligons, Nv, from 3 to 50, generating 1000 tessellations for each Nv."

L. 297: "$\beta = 2/3$ b": I think this should be "   = b. ln(10)", which is ~2.3 b.

Yes thanks, it was an oversight. It is "= b. ln(10)" because we are taking into account the equation with magnitude and not seismic moment.

2.3 Combining fault and distributed sources

L. 299-300: It would be better to describe this concept before the two source model components are described (see general remark).

Thanks for the suggestion. We'll introduce this concept before in the manuscript.

L. 307: Add some statement that this assumption is explained in more detail in the following paragraphs.

Ok, at the end of the line 307 we'll add a sentence as:"… this assumption is explained in more detail further on."

L. 338-340: Is this valid for all types of faults or only for dip-slip faults?

It is valid only for dip-slip faults, and because we want be more general with this concept, we'll modify the lines 338-340 as: "Static stress changes produce areas of negative stress, also known as shadow zones, and positive stress zones".

L. 360: Perhaps add that it is a linear function.

Ok, we'll add it. We'll modify line 360 in: "we introduced a slip rate and a distance-weighting linear function.."

L. 363: Write the equation more completely:

We'll, thanks.

However, there is still a problem with the second line, which does the opposite of what is intended (going to 1 as d increases): instead of 1/d it should be d/d_{max}…

Thanks, you are right, we'll correct.

L. 366-367: What is the rationale for varying d_{max} in function of slip rate?

We made a simple assumption, higher is the slip rate, higher is the deformation field and so higher is the value of d_{max}. We'll explain our rationale in the manuscript.

L. 369-371: This is hard to understand. Maybe rephrase as "Because we considered two fault source models, one using only TGR MFDs and the other only CHR MFDs, and because the MFDs of distributed seismicity grid points in the vicinity of faults are modified with respect to the MFDs of these faults, we also obtain two different models of distributed seismicity."
In my opinion, it is also necessary at this point to show the summed MFDs of the different (sub)models, i.e. summed MFD of the TGR fault source model, of the CHR fault source

model, of the TGR distributed source model, of the CHR distributed source model, and of the combined TGR and CHR source models.

Thanks for the suggestion, we think that rephrasing as you suggested is clearer. As said in the previous comment, we'll add a new figure to show the MFD's of the different models.

3. Results and discussion

L. 382: "designed under the traditional Poisson hypothesis": Rephrase

We'll rephrase in: " To obtain PSH maps we assign the calculated expected seismicity rates, under Poisson hypothesis, to their pertinent geometries…"

L. 386: "well-known": this is not the most relevant property for choosing OpenQuake. Perhaps widely used, open-source, tested, …?

We'll remove "well-known" and add at line 387 before "The ground motion…" this sentence: "We used this software because it is an open source software developed recently by GEM with the purpose of providing seismic hazard and risk assessments. Moreover, it is widely recognized within the scientific community for its potential."

L. 402: Explain more explicitly that the TGR and CHG fault source models are end members that are only used to explore the epistemic uncertainty, and that in the preferred fault source model a choice is made between the two MFD models for each fault.

Thanks for your suggestion; we'll better explain our choices.

L. 403-404: "Although both models have the same amount of seismic moment release": this has not been demonstrated.

Here, we were discussing about the two fault source models. In this case the same amount of seismic moment release is an assumption that we made before to compute the MFD's, as before explained.

L. 409-411: "The rates of earthquakes with magnitudes between 5.5 and approximately 6, …, are generally higher in the TGR model than in the CHG model": Please demonstrate by showing the summed MFDs.

Will be shown in a new figure (now Figure S2 in the supplement).

L. 443: “a magnitude lower or higher than the bell curve” → “a magnitude lower or higher than the magnitude range in the bell curve”. See also my remark at lines 197-198: a higher magnitude should not be possible!

We’ll improve the manuscript, better describing our approach: see the answer in the general comments.

L. 468-471: It has not been explained exactly how the TGR MFDs have been constructed. See my remark at lines 209-211.

We’ll add this information at line 209-211. See our reply at these lines.

L. 505: Perhaps replace “TGR model” with a brief description like you do for the CHG model in the following line.

Thanks for your comment, we agree. We’ll add at line 505 a sentence as:” the Truncated Gutenberg-Richter model, where the maximum magnitude is the upper threshold and M_w *= 5.5 is the lower threshold for all faults…”.*

4. Conclusions

L. 558-559: “pattern similar to that of the current national maps at the national scale, but some significant differences in hazard are present at the regional-to-local scale”: this has not been discussed in the main text. It would be instructive to show both maps side by side and describe the comparison in some more detail in §3.

See our reply at general comments and the new figure (now Figure S1 in the supplement). As suggested, the new figure we’ll be included in the manuscript, at Chapter 3.

L. 563-565: See my comment for lines 409-411. It would also be interesting to compare the summed MFDs to the observed MFD based on the full catalog, to see which of the two MFD models is closer to the observations in this particular magnitude range (M 5.5 to ~6.0).

See our reply at general comments and the new figure (now Figure S2 in the supplement).

Figure captions

Fig. 9 : Explain acronym "poe"

In the caption we’ll add this sentence: ”The dashed lines represent the 2%, 10% and 81% probability of exceedance (poe) in 50 years.”

Fig. 12: How are the contributions of the component source models computed? The perfect symmetry between the contributions of the fault source model and the distributed source model gives me the impression that they do not correspond to the contributions one would obtain from a deaggregation.

Yes, you're right it is not a deaggregation. It is the contribution of each source model in the total. For example, if the PGA value in a given point of the grid is: 0.15, 0.20 and 0.35 for the distributed, fault source and total respectively, the contribution will be 43% and 57% for the distributed and fault source respectively. Probably could be right to better explaining this in the manuscript, and so at line 482 we'll add a sentence as: "Note that the contributions are not given by deaggregation but are computed how the percentage of each source model in the PGA value of the total model."

Cited papers

Basili, R., G. Valensise, P. Vannoli, P. Burrato, U. Fracassi, S. Mariano, M. M. Tiberti, and E. Boschi. 2008. 'The Database of Individual Seismogenic Sources (DISS), version 3: Summarizing 20 years of research on Italy's earthquake geology', Tectonophysics, 453: 20-43.

Boncio, P., Brozzetti, F. and Lavecchia G. 2000. Architecture and seismotectonics of a regional Low-Angle Normal Fault zone in Central Italy. Tectonics, 19 (6), 1038-1055

Pace, B., F. Visini, and L. Peruzza. 2016. 'FiSH: MATLAB Tools to Turn Fault Data into Seismic- Hazard Models', Seismological Research Letters, 87: 374-86.

Review of manuscript NHESS-2017-41 "Integrating faults and past earthquakes into a probabilistic seismic hazard model for peninsular Italy" by Alessandro Valentini, Francesco Visini & Bruno Pace

by Laurentiu Danciu
Swiss Seismological Service
ETH Zurich

General Comments

The manuscript provides a procedure to integrate active faults in a regional seismogenic source model for Italy. A database of active faults was compiled and fully parameterised for use together with observed seismicity (instrumental and historical) to forecast the spatial and temporal distribution of future seismicity. Earthquake recurrence models of the delineated active faults are model by two magnitude-frequency distributions: either a Characteristic Gaussian (CHG) or Truncated Gutenberg-Richter (TGR). Additionally, the seismicity off faults is described by a smoothed seismicity using a complete earthquake catalogue of the region. The two models are complementary not independent, thus the earthquake rates account for double-counting of earthquakes assigned to faults above specified threshold magnitude. Further, a novel weighting function to correct the earthquake rates in vicinity of fault sources is proposed and used. The resulting two seismic sources are eventually combined in a mixed source model representing the suitable activity rates in time and space. The authors conclude with a sensitivity analysis evaluating the impact of the two models of earthquake recurrence rates on the total seismic hazard.

The use of active faults in seismic hazard assessment has become extensive in the last decades due to efforts of data compilation and analysis. Active faults provides the information to extend the observational time of large magnitude earthquakes which often is not captured by the existing catalogues of observed seismicity. The current manuscript provides a step forward into this direction. The combination active faults and smoothed seismicity is not a novel procedure but rather state of practice. Overall, the manuscript is relatively well written, there are several misleading parts to be improved, highlighted in my detailed comments. The structure of the manuscript is consistent with the procedural steps and no major changes are required. The figures, tables and supplemental materials are clear and appropriated. There are some key references missing but this is not necessarily a criticism. The conclusions appear appropriate with the proposed procedure and analysed content. My comments follow the structure of the manuscript and summarised below:

1. First and foremost the authors should be clearly state that this is not an update of the seismic hazard model of Italy, and that the purpose of the study is to integrate the active faults in a hazard calculation. Moreover, the resulting seismogenic model presented in this study has limitations, such as the use only of shallow faults, but not the subduction and volcanic sources.

   To clearly state that our model is not aimed to update seismic hazard model of Italy, we will add at line 70 the following statement: "In conclusion, even if the main purpose of this work is to integrate the active faults in a hazard calculation for the Italian territory, this work does not represent an official update of the seismic hazard model of the Italy".
   About the use of only shallow faults, but not the subduction and volcanic sources, we will more clear introduce this issue in the manuscript. In any case in this paper we want to focus on the

impact of the integration of faults and earthquakes data, without the assumption to be complete in terms of fault database, but on the contrary suggesting a way to integrate two incomplete database in the best way, without throwing data.

2. A definition of active fault in the context of the study must be introduced. The literature distinguishes between active faults in geological time, i.e. Quaternary or Neocene, capable of future reactivation. Moreover, the slip rate assumptions must be discussed. It is well accepted that large variability are associated with the slip-rate values, and some portion of slip-rate can be aseismic. Extension of this discussion must be introduced in the context of this study.

   We agree that a definition of active fault in the context of the study is necessary. We will add at line 82 a phrase as: "For seismic hazard assessment an active fault is a structure that has evidence of activity in the late Quaternary (i.e. in the past 125 kyr), a demonstrable or potential capability of generating major earthquakes and capable of future reactivation (see Machette, 2000 for a discussion on terminology). The evidences of quaternary activity can be geomorphological and/or paleoseismological, when activation during instrumental seismic sequences and/or association to historical earthquakes are not available".
   We will also extend discussion about slip rates assumptions for PSHA. In particular, we will more clear to state that we are assuming that slip-rates used are representative of seismic movements (no-aseismic factor). We think that investigating the impact of this assumption could be an issue of uncertainty-focused paper, for example by differentiating aseismic slip factor in respect to different tectonic contests.

3. Further, the authors are aware of the 2013 European Seismic Hazard Model (ESHM13, Woesner et al 2015) developed within the SHARE Project. It might be worth discussing the two approaches side by side, as the ESHM13 is the first reference model to introduce active faults for Euro-Mediterranean Region.

   We prepared a new figure (Figure S1 in supplement) to compare our model, FSBG model proposed by SHARE and the Italian seismic hazard map MPS04, using the same GMPE's. A discussion about this comparison will be added in the "Results and Discussion" chapter.

4. There are several procedural steps that are not well explained in the document, such as the estimation of the activity rates for faults. Albeit, the main focus of the procedure is to implement active faults to seismic hazard, the activity rates are yet described as input to the FiSH code and the segment seismic moment conservation. In my opinion this is not enough. The key elements and assumptions for computing the activity rates of active faults needs more attention, supported with discussions of the sensitivity of the input parameters, i.e. the effect of slip rates to earthquake recurrence rates.

   In order to explain more in detail the segment seismic moment conservation, we will modify part of the text by adding the following paragraph:
   "… which divides the seismic moment that corresponds to Mmax by the moment rate given a slip rate:

$$T_{mean} = \frac{1}{Char\_Rate} = \frac{10^{1.5M_{max}9.1}}{\mu VLW}$$

where Tmean is the mean recurrence time in years, Char_Rate is the annual mean rate of occurrence, Mmax is the computed mean maximum magnitude, μ is the shear modulus, V is the average long-term slip rate, and L and W are the geometrical parameters of the fault, along-strike rupture length and down dip width respectively."

Moreover, to explain how magnitude frequency distribution of TGR is computed we will state that: " For MFD, the b-value is constant and equal to 1.0 for all faults, obtained by the interpolation of the earthquakes in the CPTI15 catalogue, as the events on the single sources are insufficient for statistics. However the a-values have been computed by Activity Rate FiSH code, balancing the total expected seismic moment rate with the seismic moment rate that was obtained by the pair Mmax and Tmean, evaluated by the fault geometry and the slip rate of each individual source (details in Pace et al., 2016)."

5. The role of each magnitude frequency distribution (MFD) for each fault is not clear as described in the current version. One might expect a logic tree of the two MFDs. This aspect needs to be emphasised in the introduction.

Thanks for your suggestion. We'll clarify in the Introduction our choices, explaining that the TGR and CHG MFD are here used as end members, in order to explore the epistemic uncertainties, and we consider the Mixed model as a sort of an "expert judgment" model, useful for comparison analysis. As our model is not aimed to update seismic hazard model of Italy, we don't think we need to use a logic tree approach to produce a weighted model.

6. Maximum magnitude assigned to each fault based on empirical magnitude scaling relationships do not account for uncertainties of the fault size (subsurface length or area). From the current version of the manuscript it is not evident the error associated to the fault size in the fault dataset.

In our work, the error associated to the fault size was not taken into account because there are no indications to quantify these errors from the published data used to obtain the active fault database. The error associated to the Mmax of the fault sources is only based on the errors of the used empirical relationships and observations.

7. Also, one can argue that more recent magnitude scaling relationships can be used (e.g Leonard et al 2010) but for those used, the role of aleatory uncertainty must be mentioned and quantified herein. The authors should describe the procedure implemented in the FiSH code because not everyone has access to that manuscript.
8. Five maximum magnitude values are described as being assigned to each fault. The way these five values are implemented in the final computational model is not clear. Are these values modelled in a logic tree?

We will add a description of the procedure to estimate Mmax for faults after summarizing what has been done in Pace et al. (2016) FiSH code: "Because all the empirical relationships and observations are affected by uncertainties, a first code (MB) is designed to take these factors into *account and return a maximum magnitude value and a standard deviation. The uncertainties in the empirical scaling relationship are taken from the studies of Wells and Coppersmith (1994), Peruzza and Pace (2002) and Leonard (2010). Currently, the uncertainty in magnitude from seismic moment is fixed and set to 0.3, whereas the uncertainty in Mobs is defined by the catalogue. To combine the maximum magnitudes, MB draws a probability curve for each magnitude estimate by assuming a normal distribution. It is possible to define the number of standard deviations (σ) for truncating the normal distribution of magnitudes at both sides. MB successively sums the probability density curves and fits the summed curve to a normal distribution to obtain the mean of the maximum magnitude Mmax and its standard deviation. Therefore, Mmax represents an evaluation of the maximum rupture that is allowed by the fault geometry and the rheological properties".*

9. A sensitivity analysis to the choice of the maximum magnitude may be necessary to explain the effect of maximum magnitude for the TGR. For the same slip rate increase of the maximum magnitude will result in a decrease of the recurrence of small events. This effect is due to the fact that the largest earthquake accounts for most of the seismic moment and this requires the subtraction of small events to maintain the seismic moment balance.

   We agree with the topic here raised by the reviewer. Actually, the impact of uncertainties in Mmax and slip rate into PSHA is an important question, but we think it deserves a more extensive work to be exhaustively pointed out. We prepared a figure to show how varying these two parameters the seismicity rates can be distributed following a TGR model (Figure S3 in supplement). In our paper only the central values of the shown MFDs has been used. It is clear the final PSHA is substantially modified when Mmax and slip rate are changed, but, for the purpose of our work, this aspect is out of topic. We are exploring these (and other) aspects of fault-based approaches but, again, to be at least sufficiently analysed, they should be ingredients for a new work.

10. In a general way, the characteristic model implies a recurrence rate estimated on large past large-magnitude earthquakes recognised from past geological record and the time interval between events can be measured. How many of the faults have a geological record long enough to characterise the recurrence of the large magnitude events? In the current version of the manuscript the historical events are linked to the faults, thus the long-term representation of the fault activity is questionable.

    Thanks for your comment, we were not clear in explain how the mean recurrence times (Tmean) of the characteristic earthquake have been calculated. Similarly to TGR MFD we evaluated Mmax and Tmean by the fault geometry and the slip rate (not with the observed occurrences) of each individual source and we calculated the total expected seismic moment rate (eq. in the answer to comment 4). Then, we partitioned the total expected seismic moment rate in a range given by Mmax +- 1 standard deviation following a Gaussian bell distribution. We'll improve the manuscript to better explain this concept.

11. Slip rates are averaged over successive geologically recognised earthquakes and prone to error in measurements, hence the uncertainties of the slip-rates needs to be quantified.

    Uncertainties in slip rates estimates are given in the seismogenic sources database in the appendix. For our PSHA model we used the central value of the slip rate range given for each *fault. We are assuming that this value is representative of the average long term behaviour of the fault. Unfortunately, the state of the art of the knowledge of slip rates in Italy cannot allows to resolve a more detailed analysis of slip rate. However, varying slip rates in the currently range of uncertainty (as published in the papers cited in the appendix), we produced the figure S3 (in the supplement) to show the impact of these uncertainties on the activity rates.*

12. When combining active faults and background seismicity, it is mandatory a comparison of the seismic productivity (CHG and TRT) of the faults with the gridded seismicity in the vicinity of faults. Without such comparison it is difficult to assess the performance of the models.

    Thanks for your suggestion. We attach in supplement a new figure (Figure S2) showing and comparing the summed MFD's of the fault source inputs (TGR, CHG, Mixed), the distributed source input, the final model (distributed + fault) and the CPTI15 catalogue. This new figure shows, in a sector of Italy where the faults are well defined, the behaviour of the activity rates as derived by our approach. The new figure we'll be included in the revised version of the manuscript.

13. Generally, evaluating the performance of seismogenic sources based on seismic hazard estimates is not recommended. The hazard estimates based on active faults only is misleading, as the active faults are incomplete in space, and not treated as independent models. Thus the model performance may be evaluated at the level of seismicity rates comparison, not for hazard estimates.

    Thanks for your comment, we agree it is important, in order to evaluate the performance of different seismic models for seismic hazard, a direct comparison of seismicity rates. For this reason we'll add in the manuscript the figure above described (Figure S2 in supplement). In any case we think it is interesting to show the impact of different seismogenic sources also in terms of seismic hazard maps.

14. The authors should state clearly that a suitable seismogenic source model combines the active faults and the gridded seismicity as mixed model.

    As also commented later, we agree that a model should include faults and distributed sources. We will clearly state that the mixed fault source is obtained by our judgment on the MFD assigned to each single fault, and that the mixed model combines this fault source input with the distributed sources input.

Section Specific Comments

L50:51: "In Europe, a working group…" In Europe, within the SHARE project (Giardini et al 2010) has introduced the use of active faults at the region level for the first time. I am surprised that the authors do not refer in their study to the fault source models for Italy, the DISS (Database of Individual Seismogenic Sources). What are the main similarities and differences between the two dataset? The authors may consider adding a reference and a discuss the two datasets to avoid confusion.

We mentioned SHARE project in our manuscript at line 58, and a new figure (S1 in supplement) compares the results. About the DISS, we will at line 84: "Although for the Italian territory there is already a database that contains the results of the investigations of the active tectonics during the past 20 years (Database of Individual Seismogenic Sources, DISS, http://diss.rm.ingv.it/diss/), made by three main categories of seismogenic sources: individual seismogenic sources, seismogenic areas, macroseismic sources, it does not work well to elaborate a PSHA model using individual seismogenic sources, as in this work. In fact, the DISS Authors (Basili et al., 2008) say that the individual seismogenic sources database cannot guarantee the completeness of the sources themselves and are not meant to comprise a complete input dataset for probabilistic assessment of seismic hazard. For this reason, we are not restricted to just use of the DISS, but trough a synthesis of published works over the last twenty years (see supplements for complete references) we defined a database as complete as possible, in terms of individual seismogenic sources, and parameters to have input dataset for PSHA."

L63: 66 The uniform seismotectonic sources of the Italian hazard described by Stuchi et al (2011) are delineated considering the fault information where and when available. The more realistic pattern of ground motion due to faults it is questionable, because an area source delineated to describe a group of faults, it will produce a similar pattern with the individual faults. The major benefits of using the active faults is to extend the observational time to capture the recurrence of large magnitude events. The local pattern due to fault location might be controlled by other factors such as hanging wall, upper seismogenic depth, style of faulting. However, these effects are not evident if an inappropriate ground motion model is selected. Thus the seismic hazard pattern depends on both seismic source representation and ground motion models.

We will modify from line 65: "…in order to obtain more detailed patterns of ground motion, extend the observational time to capture the recurrence of large magnitude events, and to improve the reliability of seismic hazard assessments." Moreover, we will add a new figure (Figure S1 in supplement) to compare the MPS04 and our PSHA model

L72. The term models is misleading. A source model implies a complete source representation in space and time aimed at describing the seismogenic potential of the region. In the current context, the active faults are incomplete in space, they are not describing all the tectonics of the region - not volcanic, subduction or deep seismicity reported for the Italian territory. It has to be specified that these are individual seismic sources, but not independent models. The procedure proposed here is aiming at creating a "model" for an exercise of seismic hazard evaluation. Moreover, if the goal of the work is to provide a robust seismic hazard estimates, then the authors resolve the issues of model independence and completeness as well as to capture the epistemic uncertainties in the mixed source model.

We agree with your comment, and so following your suggestion we'll remove the term "model" when we describe the fault source geometry, while we'll maintain the term "model" when we combine fault and distributed sources for the seismic hazard evaluations. In any case we want to highlight that the main aim of this work is how to combine fault and distributed sources in order to take into account and possibly overcome the incompleteness of the fault source database, without throwing data. We will add in the manuscript a phrase explaining our choices.

L120: The time scale is a key aspect to evaluate the long-term representation of the seismic productivity of active faults. If a fault has moved in the recent geologically time , i.e Holocene, it might be considered as seismically active, if it moved in the far-off geologic time and has not moved again since then the fault might be judged to be an inactive fault. Hence, it might be of interest to specify the time scale and the definition of active faults on the present investigation. Yet, as mentioned before there is need to clarify the definition of fault activity or non activity.

Please see our comment above on active fault definition (remark n. 2).

L131:135. The slip rate values for some faults are very low. Values of 0.3 mm/year are extremely low and the movement on these faults could also takes place as creep. Is the aseismic factor adjusting the slip rates? Are these slip-rates supported by historical seismicity observations, geological investigations and /or paleoseismicity studies?

These slip-rates are supported by historical seismicity observations, geological investigations and /or paleoseismicity studies as reported in the supplement files. Moreover we are assuming that the used slip-rates are representative of seismic movements (no-aseismic factor), as discussed above (remark n.2).

L152: The name could be “Segmentation rules for delineating (or aggregating) fault sources”

Thanks for the suggestion, we will modify it.

L199: The role of aspect ratio must be discussed in greater extend than currently version. The extension along-strike dimensions of the faults seems to be constrained by this parameter.

We will rephrase from line 199 as: ”…by reducing the fault length if the aspect ratio (W/L) is smaller than indicated by the relation between aspect ratio and rupture length for observed earthquake ruptures as derived by Peruzza and Pace (2002).”

L191: There are five Mmax values for each fault. How is the Mmax modelled in the hazard calculation?

Please, see the comment to remark n. 8

L202: Introduce and explain the “segment seismic moment conservation”? The key assumptions and the input parameters of the recurrence rates must be described. Characterisation of the active faults is a key aspect of this approach, thus it requires more description. As mentioned before, the effect of maximum magnitude must be discussed. In the case of seismic moment balance, for a constant slip rate, the recurrence rates of small events are decreasing with increased magnitude.

We will introduce and explain better this issue. Please, see the replies to remarks n. 2, 4, and 9.

L207:211: What is the rationale of the two MFDs? It is not evident why the two recurrence models are selected? In a general way, the characteristic earthquake is used to define an earthquake of a given magnitude and well identified recurrence time by geological evidences. The fault sources used here do not qualify for such model, for various reasons including the way they are constructed by linkage of various segments. A characteristic model will be appropriate for use on individual segment rather than a long composite fault. See discussions of Kagan (1993), that clearly states that the evidence of the characteristic earthquake hypothesis can be explained either by statistical bias or statistical artifact. Thus, it will be of great interest for the readers to specify the assumptions for the two MFDs.

We agree that it is difficult to define an appropriate MFD (e.g. characteristic earthquake) for individual source using the available geological data, and important project as UCERF3 didn't solve the same doubts. In any case our fault source database have been developed to be representative of the maximum single earthquake rupture, and not long composite faults, by using restrictive segmentation rules described in chapter 2.1.2. Moreover, the two MFD are used as end members, in order to explore the epistemic uncertainties, and we consider the Mixed model as a sort of an "expert judgment" model, useful for comparison analysis.

L278: the number of Voronoi polygons is not clear to me. There are 3 to 50 polygons across the entire region? Each polygon is tectonic dependent? Please clarify.

We will modify the manuscript from the line 276: "… the Voronoi tessellation of space without tectonic dependency. The whole Italian territory has been divided into a grid with a longitude/latitude spacing of 0.05°, and the centres of the grid cells represent the possible centres of Voronoi polygons. We vary the number Voronoy polygons, Nv, from 3 to 50, generating 1000 tessellations for each Nv."

L286: Who is parametrised the depth and the maximum magnitude for gridded seismicity? Are these parameters treated as aleatory or epistemic?

The parameters have been taken from SHARE project, as written at lines 285-291. We did not explore the variability of these parameters.

L382: For the purpose of an exercise one GMPE might have been justified. However, the focus of the study should be the comparison of the earthquake recurrence rates not the hazard estimates.

We believe that the use of these GMPE's is correct, as they have been developed for Active Crust regions. Comparing model in terms of rates is for sure a valid approach. However, as the aim of our work is a PSH model, we believe that comparing different model (using the same GMPE's) can be useful. In any case we'll add in the manuscript a figure comparing the results also in terms of activity rates (Figure S2 in supplement).

Cited papers

Basili, R., G. Valensise, P. Vannoli, P. Burrato, U. Fracassi, S. Mariano, M. M. Tiberti, and E. Boschi. 2008. 'The Database of Individual Seismogenic Sources (DISS), version 3: Summarizing 20 years of research on Italy's earthquake geology', *Tectonophysics*, 453: 20- 43.

Leonard, M. (2010). Earthquake fault scaling: Self-consistent relating of rupture length, width, average displacement, and moment release. *Bulletin of the Seismological Society of America*, *100*(5A), 1971-1988.

Machette, M.N., 2000, Active, capable, and potentially active faults; a paleoseismic perspective, *J. Geodyn.* **29**, 387–392.

Pace, B., F. Visini, and L. Peruzza. 2016. 'FiSH: MATLAB Tools to Turn Fault Data into Seismic-Hazard Models', Seismological Research Letters, 87: 374-86.

Peruzza, L., and B. Pace. 2002. 'Sensitivity analysis for seismic source characteristics to probabilistic seismic hazard assessment in central Apennines (Abruzzo area) '. Bollettino di Geofisica Teorica ed Applicata 43, 79–100.

Wells, D. L., and K. J. Coppersmith. 1994. 'New Empirical Relationships among Magnitude, Rupture Length, Rupture Width, Rupture Area, and Surface Displacement', Bulletin of the Seismological Society of America, 84: 974-1002.

Woessner, J., D. Laurentiu, D. Giardini, H. Crowley, F. Cotton, G. Grunthal, G. Valensise, R. Arvidsson, R. Basili, M. B. Demircioglu, S. Hiemer, C. Meletti, R. W. Musson, A. N. Rovida, K. Sesetyan, M. Stucchi, and SHARE Consortium. 2015. 'The 2013 European Seismic Hazard Model: key components and results', Bulletin of Earthquake Engineering, 13: 3553-96

Integrating faults and past earthquakes into a probabilistic seismic hazard model for peninsular Italy

Alessandro Valentini[1], Francesco Visini[2] and Bruno Pace[1]

[1] DiSPUTer, Università degli Studi "Gabriele d'Annunzio", Chieti, Italy

[2] Istituto Nazionale di Geofisica e Vulcanologia, L'Aquila, Italy

Abstract

Italy is one of the most seismically active countries in Europe. Moderate to strong earthquakes, with magnitudes of up to ~7, have been historically recorded for many active faults. Currently, probabilistic seismic hazard assessments in Italy are mainly based on area source models, in which seismicity is modelled using a number of seismotectonic zones and the occurrence of earthquakes is assumed uniform. However, in the past decade, efforts have increasingly been directed towards using fault sources in seismic hazard models to obtain more detailed and potentially more realistic patterns of ground motion. In our model, we used two categories of earthquake sources. The first involves active faults, and fault slip rates were used to quantify the seismic activity rate. We produced an inventory of all fault sources with details of their geometric, kinematic and energetic properties. The associated parameters were used to compute the total seismic moment rate of each fault. We evaluated the magnitude-frequency distribution (MFD) of each fault source using two models: a characteristic Gaussian model centred on the maximum magnitude and a Truncated Gutenberg-Richter model. The second earthquake source category involves distributed seismicity, and a fixed-radius smoothed approach and a historical catalogue were used to evaluate seismic activity. Under the assumption that deformation is concentrated along faults, we combined the MFD derived from the geometry and slip rates of active faults with the MFD from the spatially smoothed earthquake sources and assumed that the smoothed seismic activity in the vicinity of an active fault gradually decreases by a fault size-driven factor. Additionally, we computed horizontal peak ground acceleration maps for return periods of 475 and 2,475 yrs. Although the ranges and gross spatial distributions of the expected accelerations obtained here are comparable to those obtained through methods involving seismic catalogues and classical zonation models, the spatial pattern of the hazard maps obtained with our model is far more detailed. Our model is characterized by areas that are more hazardous and that correspond to mapped active faults, while previous models yield expected accelerations that are almost uniformly distributed across large regions. In addition, we conducted sensitivity tests to

Authors 28/8/y 12:12
Formattato: Tipo di carattere:Inglese (Regno Unito)

Authors 28/8/y 12:12
Eliminato: *on*

Authors 28/8/y 12:12
Eliminato: *of*

Authors 28/8/y 12:12
Eliminato: *in historical times*

Authors 28/8/y 12:12
Eliminato: *the*

Authors 28/8/y 12:12
Eliminato: *on*

Authors 28/8/y 12:12
Eliminato: *to be*

Authors 28/8/y 12:12
Eliminato: *l*

Authors 28/8/y 12:12
Eliminato: *possibly*

Authors 28/8/y 12:12
Eliminato: *,*

Authors 28/8/y 12:12
Eliminato: *on*

Authors 28/8/y 12:12
Eliminato: *a*

Authors 28/8/y 12:12
Eliminato: *for*

Authors 28/8/y 12:12
Eliminato: *distributions*

Authors 28/8/y 12:12
Eliminato: *,*

Authors 28/8/y 12:12
Eliminato: *earthquakes*

Authors 28/8/y 12:12
Eliminato: *earthquakes*

Authors 28/8/y 12:12
Eliminato: *-*

Authors 28/8/y 12:12
Eliminato:

Authors 28/8/y 12:12
Eliminato: *We*

Authors 28/8/y 12:12
Eliminato: *the*

determine the impact on the hazard results of the earthquake rates derived from two MFD models for faults and to determine the relative contributions of faults versus distributed seismic activity. We believe that our model represents advancements in terms of the input data (quantity and quality) and methodology used in the field of fault-based regional seismic hazard modelling in Italy.

1. Introduction

In this paper, we present the results of a new probabilistic seismic hazard (PSH) model for Italy that includes significant advances in the use of integrated active fault and seismological data. The use of active faults as an input for PSH analysis is a consolidated approach in many countries characterized by high strain rates and seismic releases, as shown, for example, by Field et al. (2015) in California and Stirling et al. (2012) in New Zealand. However, in recent years, active fault data have also been successfully integrated into PSH assessments in regions with moderate-to-low strain rates, such as SE Spain (e.g., Garcia-Mayordomo et al., 2007), France (e.g., Scotti et al., 2014), and central Italy (e.g., Peruzza et al., 2011).

In Europe, a working group of the European Seismological Commission, named *Fault2SHA*, is discussing fault-based seismic hazard modelling (https://sites.google.com/site/linkingfaultpsha/home). The working group, born to motivate exchanges between field geologists, fault modellers and seismic hazard practitioners, organizes workshops, conference sessions, and special issues and stimulates collaborations between researchers. The work we are presenting here stems from the activities of the *Fault2SHA* working group.

Combining active faults and background sources is one of the main issues in this type of approach. Although the methodology remains far from identifying a standard procedure, common approaches combine active faults and background sources by applying a threshold magnitude, generally between 5.5 and 7, above which seismicity is modelled as occurring on faults and below which seismicity is modelled via a smoothed approach (e.g., Akinci et al., 2009), area sources (e.g., the so-called FSBG model in SHARE; Woessner et al., 2015) or a combination of the two (Field et al., 2015; Pace et al., 2006).

Another important issue in the use of active faults in PSHA is assigning the “correct” magnitude-frequency distribution (MFD) to the fault sources. Gutenberg-Richter (GR)

Authors 28/8/y 12:12
Eliminato: *magnitude-frequency distribution*

Authors 28/8/y 12:12
Formattato: Tipo di carattere:Non Corsivo

Authors 28/8/y 12:12
Formattato: Tipo di carattere:Non Corsivo

Authors 28/8/y 12:12
Eliminato: *think*

Authors 28/8/y 12:12
Eliminato: *an advance for Italy*

Authors 28/8/y 12:12
Eliminato: *the*

Authors 28/8/y 12:12
Eliminato: in seismic hazard estimations.

Authors 28/8/y 12:12
Eliminato: by

Authors 28/8/y 12:12
Eliminato: In Europe, a working group of the European Seismological Commission, named *Fault2SHA*, has recently discussed fault-based seismic hazard modelling (https://sites.google.com/site/linkingfaultpsha/home).

Alessandro 28/8/y 13:15
Commenta [1]: After Editor comment

Authors 28/8/y 12:12
Eliminato: Combining seismic hazards from active faults with background sources is also

Authors 28/8/y 12:12
Eliminato: .

Authors 28/8/y 12:12
Eliminato:

Authors 28/8/y 12:12
Eliminato: Currently

and characteristic earthquake models are commonly used, and the choice sometimes depends on the knowledge of the fault and data availability. Often, the choice of the “appropriate” MFD for each fault source is a difficult task because palaeoseismological studies are scarce, and it is often difficult to establish clear relationships between mapped faults and historical seismicity. Recently, Field et al. (2017) discussed the effects and complexity of the choice, highlighting how often the GR model results are not consistent with data; however, in other cases, uncharacteristic behaviour, with rates smaller than the maximum, are possible. The discussion is open (see for example the discussion by Kagan et al., 2012) and far from being solved with the available observations, including both seismological and/or geological/paleoseismological observations. In this work, we explore the calculations of these two MFDs, a characteristic Gaussian model and a Truncated Gutenberg-Richter model, to explore the epistemic uncertainties and to consider a *Mixed model* as a so-called “expert judgement” model. This approach is useful for comparative analysis, and which we assigned one of the two MFDs to each fault source. The rationale of the choice of the MFD of each fault source is explained in detail later in this paper. However, this approach obviously does not solve the issue, and the choice of MFD remains an open question in fault-based PSHA.

In Italy, the current national PSH model for building code (Stucchi et al., 2011) is based on area sources and the classical Cornell approach (Cornell, 1968), in which the occurrence of earthquakes is assumed uniform in the defined seismotectonic zones. However, we believe that more efforts must be directed towards using geological data (e.g., fault sources and paleoseismological information) in PSH models to obtain detailed patterns of ground motion, extend the observational time required to capture the recurrence of large-magnitude events and improve the reliability of seismic hazard assessments. In fact, as highlighted by the 2016-2017 seismic sequences in central Italy, a zone-based PSH is not able to model local spatial variations in ground motion (Meletti et al., 2016), whereas a fault-based model can provide insights for aftershock time-dependent PSH analysis (Peruzza et al., 2016). In conclusion, even if the main purpose of this work is to integrate active faults into hazard calculations for the Italian territory, this study does not represent an official update of the seismic hazard model of Italy.

Alessandro 28/8/y 14:31
Commenta [2]: After: Editor comment; Main comment and Detailed Comments L402 by RC1; General comments number 5 and Section Specific comment L207-211 by RC2.

Authors 28/8/y 12:12
Eliminato: probabilistic seismic hazard

Authors 28/8/y 12:12
Eliminato: to be

Authors 28/8/y 12:12
Eliminato: on

Authors 28/8/y 12:12
Eliminato: think

Authors 28/8/y 12:12
Eliminato: have to

Authors 28/8/y 12:12
Eliminato: .

Authors 28/8/y 12:12
Eliminato: , obtaining more

Authors 28/8/y 12:12
Eliminato: and possibly more realistic

Authors 28/8/y 12:12
Eliminato: in order to

Authors 28/8/y 12:12
Eliminato: ly

Authors 28/8/y 12:12
Eliminato: variation of

Authors 28/8/y 12:12
Eliminato: also be give

Authors 28/8/y 12:12
Eliminato: to perform

Authors 28/8/y 12:12
Eliminato: ,

Alessandro 28/8/y 13:32
Commenta [3]: After General Comments number 1 by RC2.

2. Source Inputs

Two earthquake-source inputs are considered in this work. The first is a fault source input that is based on active faults and uses the geometries and slip rates of known active faults to compute activity rates over a certain range of magnitude. The second is a classical smoothed approach that accounts for the rates of expected earthquakes with a minimum moment magnitude (Mw) of 4.5 but excludes earthquakes associated with known faults based on a modified earthquake catalogue. Note that our PSH model requires the combination of the two source inputs related to the locations of expected seismicity rates into a single model. Therefore, these two earthquake-source inputs are not independent but complementary, in both the magnitude and frequency distribution, and together account for all seismicity in Italy.

In the following subsections, we describe the two source inputs and how they are combined in the PSH model.

2.1 Fault Source Input

In seismic hazard assessment, an active fault is a structure that exhibits evidence of activity in the late Quaternary (i.e., in the past 125 kyr), has a demonstrable or potential capability of generating major earthquakes and is capable of future reactivation (see Machette, 2000 for a discussion on terminology). The evidence of Quaternary activity can be geomorphological and/or paleoseismological when activation information from instrumental seismic sequences and/or association to historical earthquakes is not available. Fault source inputs are useful for seismic hazard studies, and we compiled a database for Italy via the analysis and synthesis of neotectonic and seismotectonic data from approximately 90 published studies of 110 faults across Italy. Our database included, but was not limited to, the Database of Individual Seismogenic Sources (DISS vers. 3.2.0, http://diss.rm.ingv.it/diss/), which is already available for Italy. It is important to highlight that the DISS is currently composed of two main categories of seismogenic sources: individual and composite sources. The latter are defined by the DISS' authors as "*simplified and three-dimensional representation of a crustal fault containing an unspecified number of seismogenic sources that cannot be singled out. Composite seismogenic sources are not associated with a specific set of earthquakes or earthquake distribution*", and

Authors 28/8/y 12:12
Eliminato: Models

Authors 28/8/y 12:12
Eliminato: models

Authors 28/8/y 12:12
Eliminato: one

Authors 28/8/y 12:12
Eliminato: model

Authors 28/8/y 12:12
Eliminato: the

Authors 28/8/y 12:12
Eliminato: one

Authors 28/8/y 12:12
Eliminato: can take into account

Authors 28/8/y 12:12
Eliminato: from

Alessandro 28/8/y 14:31
Commenta [4]: After: Main comment number 4 and Detailed Comments L233-234 by RC1

Authors 28/8/y 12:12
Eliminato: In the following subsections, we describe the two source models and how they are combined into the PSH model.

Authors 28/8/y 12:12
Eliminato: Model

Alessandro 28/8/y 14:31
Commenta [5]: After General Comment number 2 and Section Specific Comment L120 by RC2

therefore are not useful for our PSHA approach; the former is "*a simplified and three-dimensional representation of a rectangular fault plane. Individual seismogenic sources are assumed to exhibit characteristic behaviour with respect to rupture length/width and expected magnitude*" (http://diss.rm.ingv.it/diss/index.php/about/13-introduction). Even if in agreement with our approach, we note that some of the individual seismogenic sources in the DISS are based on geological and paleoseismological information, and many others used the *Boxer* code (Gasperini et al., 1999) to calculate the epicentre, moment magnitude, size and orientation of a seismic source from observed macroseismic intensities. We carefully analysed the individual sources and some related issues: (i) the lack of updating of the geological information of some individual sources and (ii) the nonconformity between the input data used by DISS in *Boxer* and the latest historical seismicity (CPTI15) and macroseismic intensity (DBMI15) publications. Thus, we performed a full review of the fault database. We then compiled a fault source database as a synthesis of works published over the past twenty years, including DISS, using all updated and available geological, paleoseismological and seismological data (see the supplemental files for a complete list of references). We consider our database as complete as possible in terms of individual seismogenic sources, and it contains all the parameters necessary to construct an input dataset for fault-based PSHA.

The resulting database of normal and strike-slip active and seismogenic faults in peninsular Italy (Fig. 1, Tables 1 and 2; see the supplemental files) includes all the available geometric, kinematic, slip rate and earthquake source-related information. In the case of missing data regarding the geometric parameters of dip and rake, we assumed typical dip and rake values of 60° and -90°, respectively, for normal faults and 90° and 0° or 180°, respectively, for strike-slip faults. In this paper, only normal and strike-slip faults are used as fault source inputs. We decided not to include thrust faults in the present study because, with the methodology proposed in this study (as discussed later in the text), the maximum size of a single-rupture segment must be defined, and segmentation criteria have not been established for large thrust zones. Moreover, our method uses slip rates to derive active seismicity rates, and sufficient knowledge of these values is not available for thrust faults in Italy. Because some areas of Italy, such as the NW sector of the Alps, Po Valley, the offshore sector of the central Adriatic Sea, and SW Sicily, may be excluded by this limitation, we are

Alessandro 28/8/y 14:30
Commenta [6]: After: Editor Comments; Main Comment number 1 by RC1; and Section Specific Comment L50-51 by RC2

Authors 28/8/y 12:12
Eliminato: Fault source models are useful for seismic hazard studies, and we define one for Italy via compilation and synthesis of neotectonic and seismotectonic data from approximately 90 published studies on 110 faults across Italy. The resulting database of normal and strike-slip active and seismogenic faults in Italy (Fig. 1, Table 1 and 2; see supplement

Authors 28/8/y 12:12
Eliminato: derived from a synthesis of published works over the last twenty years (see supplements for complete references).

Authors 28/8/y 12:12
Eliminato: for

Authors 28/8/y 12:12
Eliminato: , as

Authors 28/8/y 12:12
Eliminato: or

Authors 28/8/y 12:12
Eliminato: ,

Authors 28/8/y 12:12
Eliminato: ,

Authors 28/8/y 12:12
Eliminato: in the

Authors 28/8/y 12:12
Eliminato: model;

Authors 28/8/y 12:12
Eliminato: could

considering an update to our approach to include thrust faults and volcanic sources in a future study. The upper and lower boundaries of the seismogenic layer are mainly derived from the analysis of Stucchi et al. (2011) of the Italian national seismic hazard model and locally refined by more detailed studies (Boncio et al., 2011; Peruzza et al., 2011; Ferranti et al., 2014).

Based on the compiled database, we explored three main issues associated with defining a fault source input: the slip rate evaluation, the segmentation model and the expected seismicity rate calculation.

2.1.1 Slip rates

Slip rates control fault-based seismic hazards (Main, 1996, Roberts et al., 2004; Bull et al., 2006; Visini and Pace, 2014) and reflect the velocities of the mechanisms that operate during continental deformation (e.g., Cowie et al., 2005). Moreover, long-term observations of faults in various tectonic contexts have shown that slip rates vary in space and time (e.g., Bull et al., 2006; Nicol et al., 2006, 2010, McClymont et al., 2009; Gunderson et al., 2013; Benedetti et al., 2013, D'Amato et al., 2016), and numerical simulations (e.g., Robinson et al., 2009; Cowie et al., 2012; Visini and Pace, 2014) suggest that variability mainly occurs in response to interactions between adjacent faults. Therefore, understanding the temporal variability in fault slip rates is a key point in understanding the earthquake recurrence rates and their variability.

In this work, we used the mean of the minimum and maximum slip rate values listed in Table 1 and assumed that it is representative of the long-term behaviour (over the past 15 ky in the Apennines). These values were derived from approximately 65 available neotectonics, palaeoseismology and seismotectonics papers (see the supplemental files). To evaluate the long-term slip rate, which is representative of the average slip behaviour, and its variability over time, we used slip rates determined in different ways and at different time scales (e.g., at the decadal scale based on geodetic data or at longer scales based on the displacement of Holocene or Plio-Pleistocene horizons). Because a direct comparison of slip rates over different time intervals obtained by different methods may be misleading (Nicol et al., 2009), we cannot exclude the possibility that epistemic uncertainties could affect the original

Alessandro 28/8/y 14:32
Commenta [7]: After Detailed Comments L92 by RC1.

Authors 28/8/y 12:12
Eliminato: considered

Authors 28/8/y 12:12
Eliminato: thickness

Authors 28/8/y 12:12
Eliminato: for

Authors 28/8/y 12:12
Eliminato: in detail

Authors 28/8/y 12:12
Eliminato: model

Authors 28/8/y 12:12
Eliminato: provide a time scale with which to assess

Authors 28/8/y 12:12
Eliminato: operating

Authors 28/8/y 12:12
Eliminato: s

Authors 28/8/y 12:12
Eliminato: .

Authors 28/8/y 12:12
Eliminato: .

Authors 28/8/y 12:12
Eliminato: to

Authors 28/8/y 12:12
Eliminato: are

Authors 28/8/y 12:12
Eliminato: based on

Authors 28/8/y 12:12
Eliminato: supplement

Authors 28/8/y 12:12
Eliminato: through

Authors 28/8/y 12:12
Eliminato: for

Authors 28/8/y 12:12
Eliminato: for the same fault

Alessandro 28/8/y 14:35
Commenta [8]: After: Detailed Comment L112-124 by RC1 and General Comments number 11 by RC2.

data in some cases. The discussion of these possible biases and their evaluation via statistically derived approaches (e.g., Gardner et al., 1987; Finnegan et al., 2014; Gallen et al., 2015) is beyond the scope of this paper and will be explored in future work. Moreover, we are assuming that slip rate values used are representative of seismic movements, and aseismic factors are not taken into account. Therefore, we believe that investigating the effect of this assumption could be another issue explored in future work; for example, by differentiating between aseismic slip factors in different tectonic contexts.

Because 28 faults had no measured slip (or throw) rate (Fig. 1a), we proposed a statistically derived approach to assign a slip rate to these faults. Based on the slip rate spatial distribution shown in Figure 1b, we subdivided the fault database into three large regions–the Northern Apennines, Central-Southern Apennines and Calabria-Sicilian coast–and analysed the slip rate distribution in these three areas. In Figure 1b, the slip rates tend to increase from north to south. The fault slip rates in the Northern Apennines range from 0.3 to 0.8 mm/yr, with the most common ranging from approximately 0.5-0.6 mm/yr; the slip rates in the Central-Southern Apennines range from 0.3 to 1.0, and the most common rate is approximately 0.3 mm/yr; and the slip rates in the southern area (Calabria and Sicily) range from 0.9 to 1.8, with the most common being approximately 0.9 mm/yr.

The first step in assigning an average slip rate and a range of variability to the faults with unknown values is to identify the most representative distribution among known probability density functions using the slip rate data from each of the three areas. We test five well-known probability density functions (*Weibull*, *normal*, *exponential*, *Inverse Gaussian* and *gamma*) against mean slip rate observations. The resulting function with the highest log-likelihood is the *normal* function in all three areas. Thus, the mean value of the *normal* distribution is assigned to the faults with unknown values. We assign a value of 0.58 mm/yr to faults in the northern area, 0.64 mm/yr to faults in the Central-Southern area, and 1.10 mm/yr to faults in the Calabria-Sicilian area. To assign a range of slip rate variability to each of the three areas, we test the same probability density functions against slip rate variability observations. Similar to the mean slip rate, the probability density function with the highest log-likelihood is the *normal* function in all three areas. We assign a value of 0.25 mm/yr to the faults

Authors 28/8/y 12:12
Eliminato: .

Alessandro 28/8/y 14:34
Commenta [9]: After Section Specific Comments L131-135 by RC2.

Authors 28/8/y 12:12
Eliminato: On the basis of

Authors 28/8/y 12:12
Eliminato: –

Authors 28/8/y 12:12
Eliminato: –

Authors 28/8/y 12:12
Eliminato: being

Authors 28/8/y 12:12
Eliminato: with

Authors 28/8/y 12:12
Eliminato: being

Authors 28/8/y 12:12
Eliminato: *Normal*, *Exponential*

Authors 28/8/y 12:12
Eliminato: *G*

Authors 28/8/y 12:12
Eliminato: lowest

Authors 28/8/y 12:12
Eliminato: N

Authors 28/8/y 12:12
Formattato: Tipo di carattere:Corsivo

Authors 28/8/y 12:12
Eliminato: for

Authors 28/8/y 12:12
Eliminato: The

Authors 28/8/y 12:12
Eliminato: *N*

Authors 28/8/y 12:12
Eliminato: N

Authors 28/8/y 12:12
Eliminato: lowest

Authors 28/8/y 12:12
Eliminato: *N*

Authors 28/8/y 12:12
Eliminato: for

Authors 28/8/y 12:12
Eliminato: the

in the northern area, 0.29 mm/yr to the faults in the Central-Southern area, and 0.35 mm/yr to the faults in the Calabria-Sicilian area.

2.1.2 Segmentation rules for delineating fault sources

An important issue in the definition of a fault source input is the formulation of segmentation rules. In fact, the question of whether structural segment boundaries along multisegment active faults act as persistent barriers to a single rupture is critical to defining the maximum seismogenic potential of fault sources. In our case, the rationale behind the definition of a fault source is based on the assumption that the geometric and kinematic features of a fault source are expressions of its seismogenic potential and that its dimensions are compatible for hosting major (Mw ≥ 5.5) earthquakes. Therefore, a fault source is considered a fault or an ensemble of faults that slip together during an individual major earthquake. A fault source is defined by a *seismogenic master fault* and its surface projection (Fig. 2a). *Seismogenic master faults* are separated from each other by first-order structural or geometrical complexities. Following the suggestions by Boncio et al. (2004) and Field et al. (2015), we imposed the following segmentation rules in our case study: (i) 4-km fault gaps among aligned structures; (ii) intersections with cross structures (often transfer faults) extending 4 km along strike and oriented at nearly right angles to the intersecting faults; (iii) overlapping or underlapping en echelon arrangements with separations between faults of 4 km; (iv) bending ≥ 60° for more than 4 km; (v) average slip rate variability along a strike greater than or equal to 50%; and (vi) changes in seismogenic thickness greater than 5 km among aligned structures. Example applications of the above rules are illustrated in Figure 2a.

By applying the above rules to our fault database, the 110 faults yielded 86 fault sources: 9 strike-slip sources and 77 normal-slip sources. The longest fault source is *Castelluccio dei Sauri* (fault number (*id in Table 1)* 42, L = 93.2 km), and the shortest is *Castrovillari* (*id* 63, L = 10.3 km). The mean length is 30 km. The dip angle varies from 30° to 90°, and 70% of the fault sources have dip angles between 50° and 60°. The mean value of seismogenic thickness (ST) is approximately 12 km. The source with the largest ST is *Mattinata* (*id* 41, ST = 25 km), and the source with the thinnest

Authors 28/8/y 12:12
Eliminato: N

Authors 28/8/y 12:12
Eliminato: model

Authors 28/8/y 12:12
Eliminato: multi-segment

Authors 28/8/y 12:12
Eliminato: the expression

Authors 28/8/y 12:12
Eliminato: to host

Authors 28/8/y 12:12
Eliminato: on

Authors 28/8/y 12:12
Eliminato: sharp bends or

Authors 28/8/y 12:12
Eliminato: one

Authors 28/8/y 12:12
Eliminato: values vary

ST is *Monte Santa Maria Tiberina* (*id* 9, ST = 2.5 km) due to the presence of an east-dipping low angle normal fault, the Alto-Tiberina Fault (Boncio et al., 2000), located a few kilometres west of the Monte Santa Maria Tiberina fault. Observed values of maximum magnitude (M_w) have been assigned to 35 fault sources (based on Table 2), and the values vary from 5.90 to 7.32. The fault source inputs are shown in Figure 3.

2.1.3 Expected seismicity rates

Each fault source is characterized by data, such as kinematic, geometry and slip rate information, that we use as inputs for the FiSH code (Pace et al., 2016) to calculate the global budget of the seismic moment rate allowed by the structure. This calculation is based on predefined size-magnitude relationships in terms of the maximum magnitude (M_{max}) and the associated mean recurrence time (T_{mean}). Table 1 summarizes the geometric parameters used as FiSH input parameters for each fault source (seismogenic box) shown in Figure 3. To evaluate M_{max} of each source, according to Pace et al., (2016) we first computed and then combined up to five M_{max} values (see the example of the Paganica fault source in Fig. 2b, details in Pace et al., 2016). Specifically, these five M_{max} values are as follows: *MM0* based on the calculated scalar seismic moment (M_0) and the application of the standard formula $M_w = 2/3\ (\log M_0 - 9.1)$ (Hanks and Kanamori, 1979; IASPEI, 2005); two magnitude values using the Wells and Coppersmith (1994) empirical relationships for the maximum subsurface rupture length (MRLD) and maximum rupture area (MRA); a value that corresponds to the maximum observed magnitude (MObs), if available; and a value (MASP, ASP for aspect ratio) computed by reducing the fault length input if the aspect ratio (W/L) is smaller than the value evaluated by the relation between the aspect ratio and rupture length of observed earthquake ruptures, as derived by Peruzza and Pace (2002) (not in the case of Paganica in Fig. 2b). Although incorrect to consider MObs a possible M_{max} value and treat it the same as other estimations, in some cases, it was useful to constrain the seismogenic potentials of individual seismogenic sources. As an example, for the *Irpinia Fault* (id 51 in Tables 1 and 2), the characteristics of the 1980 earthquake (Mw~6.9) can be used to evaluate M_{max} via comparison with the M_{max} derived from scaling relationships. In such cases, we (i) calculated the maximum expected magnitude

Alessandro 28/8/y 14:36
Commenta [10]: After Detailed Comment L180 by RC1.

Authors 28/8/y 12:12
Eliminato:).

Authors 28/8/y 12:12
Eliminato: data

Authors 28/8/y 12:12
Eliminato: 47

Authors 28/8/y 12:12
Eliminato: ,

Authors 28/8/y 12:12
Eliminato: 56

Authors 28/8/y 12:12
Eliminato: model is

Authors 28/8/y 12:12
Eliminato: s

Authors 28/8/y 12:12
Eliminato: ,

Authors 28/8/y 12:12
Eliminato: For

Authors 28/8/y 12:12
Eliminato: are computed

Authors 28/8/y 12:12
Eliminato: for

Authors 28/8/y 12:12
Eliminato:): a *MM0* value

Authors 28/8/y 12:12
Eliminato: either

Authors 28/8/y 12:12
Spostato in giù [1]: Finally, to obtain the mean recurrence time of M_{max} (i.e., T_{mean}

Authors 28/8/y 12:12
Eliminato: modifying the along-strike dimension if the rupture length exceeds the length predicted by the aspect ratio relationships (not in the case of Paganica in Fig. 2b), as derived by Peruzza and Pace (2002).

(M_{max1}) and the relative uncertainties using only the scaling relationships and (ii) compared the maximum of observed magnitudes of the earthquakes potentially associated with the fault. If MObs was within the range of M_{max} ± 1 standard deviation, we considered the value and recalculated a new M_{max} (M_{max2}) with a new uncertainty. If MObs was larger than M_{max1}, we reviewed the fault geometry and/or the earthquake-source association.

Because all the empirical relationships, as well as observed historical and recent magnitudes of earthquakes, are affected by uncertainties, the *MomentBalance* (MB) portion of the FiSH code (Pace et al., 2016) was used to account for these uncertainties. MB computes a probability density function for each magnitude derived from empirical relationships or observations and summarizes the results as a maximum magnitude value with a standard deviation. The uncertainties in the empirical scaling relationship are taken from the studies of Wells and Coppersmith (1994), Peruzza and Pace (2002) and Leonard (2010). Currently, the uncertainty in magnitude associated with the seismic moment is fixed and set to 0.3, whereas the catalogue defines the uncertainty in MObs. Moreover, to combine the evaluated maximum magnitudes, MB creates a probability curve for each magnitude by assuming a normal distribution (Fig. 2). We assumed an untruncated normal distribution of magnitudes at both sides. MB successively sums the probability density curves and fits the summed curve to a normal distribution to obtain the mean of the maximum magnitude M_{max} and its standard deviation.

Thus, a unique M_{max} with a standard deviation is computed for each source, and this value represents the maximum rupture that is allowed by the fault geometry and the rheological properties.

Finally, to obtain the mean recurrence time of M_{max} (i.e., T_{mean}), we use the criterion of "segment seismic moment conservation" proposed by Field et al. (1999). This criterion divides the seismic moment that corresponds to M_{max} by the moment rate for given a slip rate:

$$T_{mean} = \frac{1}{Char\_Rate} = \frac{10^{1.5\,M_{max}9.1}}{\mu VLW} \quad (1)$$

Alessandro 28/8/y 14:41
Commenta [11]: After Detailed Comment L197-198 by RC1.

Authors 28/8/y 12:12
Eliminato:) we use the criterion of "segment seismic moment conservation" proposed by Field et al. (1999).

Authors 28/8/y 12:12
Eliminato: Once the fault source model

Authors 28/8/y 12:12
Eliminato: calculated

Authors 28/8/y 12:12
Eliminato: rate,

Authors 28/8/y 12:12
Formattato: Tipo di carattere:Non Corsivo

Alessandro 28/8/y 14:45
Commenta [12]: After General Comments number 7 and 8 and Section Specific Comments L191 by RC2.

Authors 28/8/y 12:12
Eliminato: (Fig.

Authors 28/8/y 12:12
Spostato (inserimento) [1]

where T_{mean} is the mean recurrence time in years, Char_Rate is the annual mean rate of occurrence, M_{max} is the computed mean maximum magnitude, μ is the shear modulus, V is the average long-term slip rate, and L and W are geometrical parameters of the fault along-strike rupture length and downdip width, respectively. This approach was used for both MFDs in this study, and, in particular, we evaluated M_{max} and T_{mean} based on the fault geometry and the slip rate of each individual source. Additionally, we calculated the total expected seismic moment rate using equation 1. Then, we partitioned the total expected seismic moment rate based on a range given by M_{max} ± 1 standard deviation following a Gaussian distribution.

After the fault source is entered as input, the seismic moment rate is calculated, M_{max} (Fig. 2b) and T_{mean} are defined for each source, we computed the MFDs of expected seismicity. For each fault source, we use two "end-member" MFD models: (i) a *Characteristic Gaussian* (*CHG*) model, a symmetric Gaussian curve (applied to the incremental MFD values) centred on the M_{max} value of each fault with a range of magnitudes equal to 1-sigma, and (ii) a *Truncated Gutenberg-Richter* (*TGR, Ordaz, 1999; Kagan, 2002*) model, with M_{max} as the upper threshold and M_w = 5.5 as the minimum threshold for all sources. The b-values are constant and equal to 1.0 for all faults, and they are obtained by the interpolation of earthquake data from the CPTI15 catalogue, as single-source events are insufficient for calculating the required statistics. The a-values were computed with the ActivityRate tool of the FiSH code. ActivityRate balances the total expected seismic moment rate with the seismic moment rate that was obtained based on M_{max} and T_{mean} (details in Pace et al., 2016). In Figure 2c, we show an example of the expected seismicity rates in terms of the annual cumulative rates for the Paganica source using the two above-described MFDs.

Finally, we create a so-called "expert judgement" model, called the *Mixed* model, to determine the MFD for each fault source based on the earthquake-source associations. In this case, we decided that if an earthquake assigned to a fault source (see Table 2 for earthquake-source associations) has a magnitude lower than the magnitude range in the curve of the *CHG* model distribution, the *TGR* model is applied to that fault source. Otherwise, the *CHG* model, which peaks at the calculated M_{max}, is applied. Of course, errors in this approach can originate from the misallocation of historical earthquakes, and we cannot exclude the possibility that potentially active faults responsible for historical earthquakes have not yet been

Alessandro 28/8/y 14:45
Commenta [13]: After: Detailed Comment L202 by RC1 and General Comments number 4 and 10 by RC2.

Authors 28/8/y 12:12
Eliminato: compute the magnitude-frequency distributions

Authors 28/8/y 12:12
Eliminato: magnitude-frequency distributions

Authors 28/8/y 12:12
Eliminato: *H*

Authors 28/8/y 12:12
Eliminato: bell

Alessandro 28/8/y 14:45
Commenta [14]: After Detailed Comment L209-211 by RC1.

Authors 28/8/y 12:12
Eliminato: , following

Authors 28/8/y 12:12
Eliminato:

Authors 28/8/y 12:12
Eliminato: magnitude-frequency distributions

mapped. The MFD model assigned to each fault source in our *Mixed* model is shown in Figure 3.

2.2 Distributed Source Inputs

Introducing distributed earthquakes into the PSH model is necessary because researchers have not been able to identify a causative source (i.e., a mapped fault) for important earthquakes in the historical catalogue. This lack of correlation between earthquakes and faults may be related to (i) interseismic strain accumulation in areas between major faults, (ii) earthquakes occurring on unknown or blind faults, (iii) earthquakes occurring on unmapped faults characterized by slip rates lower than the rates of erosional processes, and/or (iv) the general lack of surface ruptures associated with faults generating M_w < 5.5 earthquakes.

We used the historical catalogue of earthquakes (CPTI15; Rovida et al., 2016; Fig. 4) to model the occurrence of moderate-to-large (Mw ≥ 4.5) earthquakes. The catalogue consists of 4,427 events and covers approximately the last one thousand years from 01/01/1005 to 28/12/2014. Before using the catalogue, we removed all events not considered mainshocks via a declustering filter (Gardner and Knopoff, 1977). This process resulted in a complete catalogue composed of 1,839 independent events. Moreover, to avoid any artificial effects related to double counting due to the use of two seismicity sources, i.e., the fault sources and the distributed seismicity sources, we removed events associated with known active faults from the CPTI15 earthquake catalogue. If the causative fault of an earthquake is known, that earthquake does not need to be included in the seismicity smoothing procedure. The earthquake-source association is based on neotectonics, palaeoseismology and seismotectonics papers (see the supplemental files) and, in a few cases, macroseismic intensity maps. In Table 2, we listed the earthquakes with known causative fault sources. The differences in the smoothed rates given by eq. (2) using the complete and modified catalogues are shown in Figure 5.

We applied the standard methodology developed by Frankel (1995) to estimate the density of seismicity in a grid with latitudinal and longitudinal spacing of 0.05°. The smoothed rate of events in each cell i is determined as follows:

Authors 28/8/y 12:12
Formattato: Tipo di carattere:Grassetto
Authors 28/8/y 12:12
Formattato: Spazio Dopo: 6 pt
Authors 28/8/y 12:12
Eliminato: Model
Authors 28/8/y 12:12
Eliminato: our
Authors 28/8/y 12:12
Eliminato: a number of
Authors 28/8/y 12:12
Eliminato: 390
Authors 28/8/y 12:12
Eliminato: the mainshock
Authors 28/8/y 12:12
Eliminato:), resulting
Authors 28/8/y 12:12
Eliminato: 621
Authors 28/8/y 12:12
Eliminato: source
Authors 28/8/y 12:12
Eliminato: the impact of
Authors 28/8/y 12:12
Eliminato: ss
Authors 28/8/y 12:12
Eliminato: has been made possible by
Authors 28/8/y 12:12
Eliminato: supplement
Authors 28/8/y 12:12
Eliminato: using
Authors 28/8/y 12:12
Eliminato: 1
Authors 28/8/y 12:12
Eliminato: the
Authors 28/8/y 12:12
Eliminato: y
Authors 28/8/y 12:12
Eliminato: on
Authors 28/8/y 12:12
Eliminato: a latitude
Authors 28/8/y 12:12
Eliminato: e

$$n_i = \frac{\Sigma_j n_j e^{\frac{-\Delta_{ij}^2}{c^2}}}{\Sigma_j e^{\frac{-\Delta_{ij}^2}{c^2}}} \qquad (2)$$

where n_i is the cumulative rate of earthquakes with magnitudes greater than the completeness magnitude Mc in each cell *i* of the grid and Δ*ij* is the distance between the centres of grid cells *i* and *j*. The parameter *c* is the correlation distance. The sum is calculated in cells *j* within a distance of 3*c* of cell *i*.

To compute earthquake rates, we adopted the completeness magnitude thresholds over different periods given by Stucchi et al. (2011) for five large zones (Fig. 4).

To optimize the smoothing distance Δ in eq. (2), we divided the earthquake catalogue into four 10-yr disjoint learning and target periods from the 1960s to the 1990s. For each pair of learning and target catalogues, we used the probability gain per earthquake to find the optimal smoothing distance (Kagan and Knopoff, 1977; Helmstetter et al., 2007). After assuming a spatially uniform earthquake density model as a reference model, the probability gain per earthquake G of a candidate model relative to a reference model is given by the following equation:

$$G = exp(\frac{L-L_0}{N}) \qquad (3)$$

where N is the number of events in the target catalogue and *L* and L_0 are the joint log-likelihoods of the candidate model and reference model, respectively. Under the assumption of a Poisson earthquake distribution, the joint log-likelihood of a model is given as follows:

$$L = \sum_{i_x=1}^{N_x} \sum_{j_y=1}^{N_y} log\ p\left[\lambda(i_x, i_y), \omega\right] \qquad (4)$$

where *p* is the Poisson probability, *λ* is the spatial density, ω is the number of observed events during the target period, and the parameters i_x and i_y denote each corresponding longitude-latitude cell.

Figure 6 shows that for the four different pairs of learning-target catalogues, the optimal smoothing distance *c* ranges from 30-40 km. Finally, the mean of all the

Authors 28/8/y 12:12
Eliminato: 1

Authors 28/8/y 12:12
Eliminato: *n*

Authors 28/8/y 12:12
Eliminato: *ni*

Authors 28/8/y 12:12
Eliminato: the

Authors 28/8/y 12:12
Eliminato: taken over

Authors 28/8/y 12:12
Eliminato: of time

Authors 28/8/y 12:12
Eliminato: 1

Authors 28/8/y 12:12
Eliminato: 2

Authors 28/8/y 12:12
Eliminato: ,

Authors 28/8/y 12:12
Eliminato: the

Authors 28/8/y 12:12
Eliminato: by the following

Authors 28/8/y 12:12
Eliminato: $[\lambda * (i_x, i_y), \omega]$

Authors 28/8/y 12:12
Eliminato: 3

Authors 28/8/y 12:12
Formattato: Tipo di carattere:Pedice

Authors 28/8/y 12:12
Eliminato: *jy*

Authors 28/8/y 12:12
Formattato: Tipo di carattere:Pedice

Authors 28/8/y 12:12
Eliminato: ,

probability gains per earthquake yields a maximum smoothing distance of 30 km (Fig. 6), which is then used in eq. (2).

The b-value of the GR distribution is calculated on a regional basis using the maximum-likelihood method of Weichert (1980), which allows multiple periods with varying completeness levels to be combined. Following the approach recently proposed by Kamer and Hiemer (2015), we used a penalized likelihood-based method for the spatial estimation of the GR b-values based on the Voronoi tessellation of space without tectonic dependency. The whole Italian territory has been divided into a grid with a longitude/latitude spacing of 0.05°, and the centres of the grid cells represent the possible centres of Voronoi polygons. We vary the number of Voronoi polygons, Nv, from 3 to 50, generating 1000 tessellations for each Nv. The summed log-likelihood of each obtained tessellation is compared with the log-likelihood given by the simplest model (prior model) obtained using the entire earthquake dataset. We find that 673 random realizations led to better performance than the prior model. Thus, we calculate an ensemble model using these 673 solutions, and the mean b-value of each grid node is shown in Figure 4.

The maximum magnitude M_{max} assigned to each node of the grid, the nodal planes and the depths have been taken from the SHARE European project (Woessner et al., 2015). The SHARE project evaluated the maximum magnitudes of large areas of Europe based on a joint procedure involving historical observations and tectonic regionalization. We adopted the lowest of the maximum magnitudes proposed by SHARE, but evaluating the impact of different maximum magnitudes is beyond the scope of this work.

Finally, the rates of expected seismicity for each node of the grid are assumed to follow the TGR model (Kagan 2002):

$$\lambda(M) = \lambda_0 \frac{\exp(-\beta M) - \exp(-\beta M_u)}{\exp(-\beta M_0) - \exp(-\beta M_u)} \qquad (5)$$

where the magnitude (M) is in the range of M_0 (minimum magnitude) to M_u (upper or maximum magnitude); otherwise $\lambda(M)$ is 0. Additionally, λ_0 is the smoothed rate of earthquakes at $M_w = 4.5$ and $\beta = b \ln(10)$.

Authors 28/8/y 12:12
Eliminato: 1
Authors 28/8/y 12:12
Eliminato: Gutenberg-Richter
Authors 28/8/y 12:12
Eliminato: time
Authors 28/8/y 12:12
Eliminato: Gutenberg-Richter's
Authors 28/8/y 12:12
Eliminato: .
Authors 28/8/y 12:12
Eliminato: centres
Authors 28/8/y 12:12
Eliminato: whole
Authors 28/8/y 12:12
Eliminato: performed
Authors 28/8/y 12:12
Eliminato: We
Authors 28/8/y 12:12
Eliminato: for
Authors 28/8/y 12:12
Eliminato: node of the
Authors 28/8/y 12:12
Eliminato: for
Authors 28/8/y 12:12
Eliminato: that depend
Authors 28/8/y 12:12
Eliminato: 4
Authors 28/8/y 12:12
Eliminato:),
Authors 28/8/y 12:12
Eliminato: , and where
Authors 28/8/y 12:12
Eliminato: 2/3
Authors 28/8/y 12:12
Eliminato: .

2.3 Combining Fault and Distributed Sources

To combine the two source inputs, we introduced a distance-dependent linear weighting function, such that the contribution from the distributed sources linearly decreases from 1 to 0 with decreasing distance from the fault. The expected seismicity rates of the distributed sources start at Mw = 4.5, which is lower than the minimum magnitude of the fault sources, and the weighting function is only applicable in the magnitude range overlapping the MFD of each fault. This weighting function is based on the assumption that faults tend to modify the surrounding deformation field (Fig. 7), and this assumption is explained in detail later in this paper.

During fault system evolution, the increase in the size of a fault through linking with other faults results in an increase in displacement that is proportional to the quantity of strain accommodated by the fault (Kostrov, 1974). Under a constant regional strain rate, the activity of arranged across strike must eventually decrease (Nicol et al., 1997; Cowie, 1998; Roberts et al., 2004). Using an analogue modelling, Mansfield and Cartwrigth (2001) showed that faults grow via cycles of overlap, relay formation, breaching and linkage between neighbouring segments across a wide range of scales. During the evolution of a system, the merging of neighbour faults, mostly along the strike, results in the formation of major faults, which are associated with the majority of displacement. These major faults are surrounded by minor faults, which are associated with lower degrees of displacement. To highlight the spatial patterns of major and minor faults, Figures 7a and 7b present diagrams from the Mansfield and Cartwright (2001) experiment in two different stages: the approximate midpoint of the sequence and the end of the sequence. Numerical modelling performed by Cowie et al. (1993) yielded similar evolutionary features for major and minor faults. The numerical fault simulation of Cowie et al. (1993) was able to reproduce the development of a normal fault system from the early nucleation stage, including interactions with adjacent faults, to full linkage and the formation of a large through fault. The model also captures the increase in the displacement rate of a large linked fault. In Figures 7c and 7d, we focus on two stages of the simulation (from Cowie et al., 1993): the stage in which the fault segments have formed and some have become linked and the final stage of the simulation.

Authors 28/8/y 12:12
Eliminato: Our PSH model requires the combination of the two source models related to the locations of expected seismicity rates into a single model. We

Authors 28/8/y 12:12
Eliminato: from

Authors 28/8/y 12:12
Eliminato: model

Authors 28/8/y 12:12
Eliminato: acts

Authors 28/8/y 12:12
Eliminato: magnitude-frequency distribution

Authors 28/8/y 12:12
Eliminato: 7).

Authors 28/8/y 12:12
Eliminato: faults located

Authors 28/8/y 12:12
Eliminato: have shown

Authors 28/8/y 12:12
Eliminato: accommodate

Authors 28/8/y 12:12
Eliminato: most

Authors 28/8/y 12:12
Eliminato: accommodate

Authors 28/8/y 12:12
Eliminato: show sketches

Authors 28/8/y 12:12
Eliminato: at

Authors 28/8/y 12:12
Eliminato: mid-point

Authors 28/8/y 12:12
Eliminato: has also shown

Authors 28/8/y 12:12
Eliminato: is

Authors 28/8/y 12:12
Eliminato: to interaction

Authors 28/8/y 12:12
Eliminato: -going

Authors 28/8/y 12:12
Eliminato: on the

Authors 28/8/y 12:12
Eliminato: whilst others remain unlinked,

Authors 28/8/y 12:12
Eliminato: last

Notably, the spatial distributions of major and minor faults are very similar in the experiments of both Mansfield and Cartwrigth (2001) and Cowie et al. (1993), as shown in Figures 7a-d. Developments during the early stage of major fault formation appear to control the location and evolution of future faults, with some areas where no major faults develop. The long-term evolution of a fault system is the consequence of the progressive cumulative effects of the slip history, i.e., earthquake occurrence, of each fault. Large earthquakes are generally thought to produce static and dynamic stress changes in the surrounding areas (King et al., 1994; Stein, 1999; Pace et al., 2014; Verdecchia and Carena, 2016). Static stress changes produce areas of negative stress, also known as shadow zones, and positive stress zones. The spatial distributions of decreases (unloading) and increases (loading) in stress during the long-term slip history of faults likely influence the distance across strike between major faults. Thus, given a known major active fault geometrically capable of hosting a Mw ≥ 5.5 earthquake, the possibility that a future Mw ≥ 5.5 earthquake will occur in the vicinity of the fault, but is not caused by that fault, should decrease as the distance from the fault decreases. Conversely, earthquakes with magnitudes lower than 5.5 and those due to slip along minor faults are likely to occur everywhere within a fault system, including in proximity to a major fault.

In Figure 7e, we illustrate the results of the analogue and numerical modelling of fault system evolution and indicate the areas around major faults where it is unlikely that other major faults develop. In Figure 7f, we show the next step in moving from geologic and structural considerations. In this step, we combine fault sources and distributed seismicity source inputs, which serve as inputs for the PSH model. Fault sources are used to model major faults and are represented by a master fault (i.e., one or more major faults) and its projection at the surface. Distributed seismicity is used to model seismicity associated with minor, unknown or unmapped faults. Depending on the positions of distributed seismicity points with respect to the buffer zones around major faults, the rates of expected distributed seismicity remain unmodified or decrease and can even reach zero.

Specifically, we introduced a slip rate and a distance-weighted linear function based on the above reasoning. The probability of the occurrence of an earthquake (Pe) with a Mw greater than or equal to the minimum magnitude of the fault is as follows:

Authors 28/8/y 12:12
Eliminato: Interestingly

Authors 28/8/y 12:12
Eliminato: to

Authors 28/8/y 12:12
Eliminato: ies

Authors 28/8/y 12:12
Eliminato: s

Authors 28/8/y 12:12
Eliminato: Earthquakes

Authors 28/8/y 12:12
Eliminato: in the hanging wall and footwall of a fault

Authors 28/8/y 12:12
Eliminato: located at the tip of the fault

Authors 28/8/y 12:12
Eliminato: along

Authors 28/8/y 12:12
Eliminato: On the other hand

Authors 28/8/y 12:12
Eliminato: schematise

Authors 28/8/y 12:12
Eliminato: from

Authors 28/8/y 12:12
Eliminato: d

Authors 28/8/y 12:12
Eliminato: for

Authors 28/8/y 12:12
Eliminato: to

Authors 28/8/y 12:12
Eliminato: to source models for

Authors 28/8/y 12:12
Eliminato: to

Authors 28/8/y 12:12
Eliminato: occurring on

Authors 28/8/y 12:12
Eliminato: a

Authors 28/8/y 12:12
Eliminato: are left

Authors 28/8/y 12:12
Eliminato: , reduced

Authors 28/8/y 12:12
Eliminato: weighting

$$Pe = \begin{cases} 0, & d \leq 1\,km \\ d/d_{max}, & 1\,km < d \leq d_{max} \\ 1, & d > d_{max} \end{cases} \qquad (6)$$

where d is the Joyner-Boore distance from a fault source. The maximum value of d (d_{max}) is controlled by the slip rate of the fault. For faults with slip rates ≥ 1 mm/yr, we assume d_{max} = L/2 (L is the length along the strike, Fig. 2a); for faults with slip rates of 0.3 - 1 mm/yr, d_{max} = L/3; and for faults with slip rates of ≤ 0.3 mm/yr, d_{max} = L/4. The rationale for varying d_{max} is given by a simple assumption: the higher the slip rate is, the larger the deformation field and the higher the value of d_{max}. We applied eq. (6) to the smoothed occurrence rates of the distributed seismogenic sources. Because we consider two fault source inputs, one using only TGR MFD and the other only CHR MFD, and because the MFDs of distributed seismicity grid points in the vicinity of faults are modified with respect to the MFDs of these faults, we obtain two different inputs of distributed seismicity. These two distributed seismogenic source inputs differ because the minimum magnitude of the faults is Mw 5.5 in the TGR model, but this value depends on each fault source dimension in the CHG model, as shown in Figure 8.

Our approach allows incompleteness in the fault database to be bypassed, which is advantageous because all fault databases should be considered incomplete. In our approach, the seismicity is modified only in the vicinity of mapped faults. The remaining areas are fully described by the *distributed* input. With this approach, we do not define areas with reliable fault information, and the locations of currently unknown faults can be easily included when they are discovered in the future.

3. Results and Discussion

To obtain PSH maps, we assign the calculated seismicity rates, based on the Poisson hypothesis, to their pertinent geometries, i.e., individual 3D seismogenic sources for the *fault* input and point sources for the *distributed* input (Fig. 8). All the computations are performed using the OpenQuake Engine (Global Earthquake Model, 2016) with a grid spacing of 0.05° in both latitude and longitude. We used this software because it is open source software developed recently by GEM with the purpose of providing seismic hazard and risk assessments. Moreover, it is widely recognized within the scientific community for its potential. The ground motion

Alessandro 28/8/y 14:47
Commenta [15]: After Detailed Comment L363 by RC1.

Authors 28/8/y 12:12
Eliminato: *Pe* = 0, when *d* ≤ 1 km; *Pe* = 1/*d*, when *d* > 1 km (5)

Authors 28/8/y 12:12
Eliminato: for

Authors 28/8/y 12:12
Eliminato: of

Authors 28/8/y 12:12
Eliminato: d

Authors 28/8/y 12:12
Formattato: Tipo di carattere:Colore carattere: Colore personalizzato(RGB(0,112,192))

Authors 28/8/y 12:12
Formattato: Tipo di carattere:Colore carattere: Automatico

Authors 28/8/y 12:12
Eliminato: 5

Authors 28/8/y 12:12
Eliminato: used

Authors 28/8/y 12:12
Eliminato: models of the magnitude-frequency distribution of

Authors 28/8/y 12:12
Eliminato: sources, i.e., the

Authors 28/8/y 12:12
Eliminato: and CHG models, we also calculated two rates of expected

Authors 28/8/y 12:12
Eliminato: for the distributed seismogenic sources.

Authors 28/8/y 12:12
Eliminato: models

Authors 28/8/y 12:12
Eliminato: model

Authors 28/8/y 12:12
Eliminato: designed under the traditional Poisson hypothesis,

Authors 28/8/y 12:12
Eliminato: expected

Authors 28/8/y 12:12
Eliminato: as described in previous sections,

Authors 28/8/y 12:12
Eliminato: *model*

Authors 28/8/y 12:12
Eliminato: *model*.

Authors 28/8/y 12:12
Eliminato: well-known

Authors 28/8/y 12:12
Eliminato: GEM

prediction equations (GMPE) of Akkar et al. (2013), Chiou et al., (2008), Faccioli et al., (2010) and Zhao et al., (2006) are used, as suggested by the SHARE European project (Woessner et al., 2015). In addition, we used the GMPE proposed by Bindi et al. (2014) and calibrated using Italian data. We combined all GMPEs into a logic tree with the same weight of 0.2 for each branch. The distance used for each GMPE was the Joyner and Boore distance for Akkar et al. (2013), Bindi et al. (2014) and Chiou et al. (2008) and the closest rupture distance for Faccioli et al. (2010) and Zhao et al. (2006).

The results of the fault source inputs, distributed source inputs, and aggregated model are expressed in terms of peak ground acceleration (PGA) based on exceedance probabilities of 10% and 2% over 50 years, corresponding to return periods of 475 and 2,475 years, respectively (Fig. 9).

To explore the epistemic uncertainty associated with the distribution of activity rates over the range of magnitudes of fault source inputs, we compared the seismic hazard levels obtained based on the TGR and CHG fault source inputs (left column in Fig. 9) using the TGR and CHG MFDs for all the fault sources (details in section 2.1.3). Although both models have the same seismic moment release, the different MFDs generate clear differences. In fact, in the *TGR* model, all faults contribute significantly to the seismic hazard level, whereas in the *CHG* model, only a few faults located in the central Apennines and Calabria contribute to the seismic hazard level. This difference is due to the different shapes of the MFDs in the two models (Fig. 2c). As shown in Figure 8, the percentage of earthquakes with magnitudes between 5.5 and approximately 6, which are likely the main contributors to these levels of seismic hazards, is generally higher in the *TGR* model than in the *CHG* model. At a 2% probability of exceedance in 50 years, all fault sources in the CHG contribute to the seismic hazard level, but the absolute values are still generally higher in the *TGR* model.

The *distributed input* (middle column in Fig. 9) depicts a more uniform shape of the seismic hazard level than that of fault source inputs. A low PGA value of 0.125 g at a 10% probability of exceedance over 50 years and a low value of 0.225 g at a 2% probability of exceedance over 50 years encompass a large part of peninsular Italy

Authors 28/8/y 12:12
Eliminato: also …sed the GMPE propos ... [1]

Authors 28/8/y 12:12
Eliminato: model… distributed source ... [2]

Authors 28/8/y 12:12
Eliminato: due to…the distribution of ac ... [3]

Authors 28/8/y 12:12
Eliminato: *model* (central …olumn in Fi ... [4]

and Sicily. Two areas with high seismic hazard levels are located in the central Apennines and northeastern Sicily.

The overall model, which was created by combining the fault and distributed source inputs, is shown in the right column of Figure 9. Areas with comparatively high seismic hazard levels, i.e., hazard levels greater than 0.225 g and greater than 0.45 g at 50-yr exceedance probabilities of 10% and 2%, respectively, are located throughout the Apennines, in Calabria and in Sicily. The fault source inputs contribute most to the total seismic hazard levels in the Apennines, Calabria and eastern Sicily, where the highest PGA values are observed.

Figure 10 shows the contributions to the total seismic hazard level by the *fault* and *distributed* source inputs at a specific site (L'Aquila, 42.400-13.400). Notably, in Figure 10, *distributed* sources dominate the seismic hazard contribution at exceedance probabilities greater than ~81% over 50 years, but the contribution of *fault* sources cannot be neglected. Conversely, at exceedance probabilities of less than ~10% in 50 years, the total hazard level is mainly associated with *fault* source inputs.

Figure 11 presents seismic hazard maps for PGAs at 10% and 2% exceedance probabilities in 50 years for *fault* sources, *distributed* sources and a combination of the two. These data were obtained using the above-described *Mixed* model, in which we selected the most "appropriate" MFD model (TGR or CHG) for each fault (as shown in Figure 3). The results of this model therefore have values between those of the two end-members shown in Figure 9.

Figure 12 shows the *CHG*, *TGR* and *Mixed* model hazard curves of three sites (Cesena, L'Aquila and Crotone, Fig. 13c). As previously noted, the results of the *Mixed* model, due to the structure of the model, are between those of the *CHG* and *TGR* models. The relative positions of the hazard curves derived from the two end-member models and the *Mixed* model depend on the number of nearby fault sources that have been modelled using one of the MFD models and on the distance of the site from the faults. For example, in the case of the Crotone site, the majority of the fault sources in the *Mixed* model are modelled using the CHG MFD. Thus, the resulting hazard curve is similar to that of the *CHG* model. For the Cesena site, the

Authors 28/8/y 12:12
Eliminato: er…seismic hazard levels ar ... [5]

Authors 28/8/y 12:12
Eliminato: total…model, which was ... [6]

Authors 28/8/y 12:12
Eliminato: 9…shows the contributions t ... [7]

Authors 28/8/y 12:12
Eliminato: 10 shows…seismic hazard n ... [8]

Authors 28/8/y 12:12
Eliminato: 8. The choice of the appropriate magnitude-frequency distribution for a fault source is a difficult task because palaeoseismological studies are scarce and it is often difficult to establish clear relationships between faults and observed seismicity. If an earthquake assigned to a fault source (see Table 2 for earthquake-source associations) has a magnitude lower or higher than the bell curve of the *CHG* model distribution, the *TGR* model is applied to that fault source. Otherwise, the *CHG* model, peaking at the calculated M_{max}, is applied. Of course, errors in this approach can originate from a misallocation of historical earthquakes, and we also cannot exclude the possibility that potentially active faults responsible for historical earthquakes have been not yet mapped. The magnitude-frequency distribution assigned to each fault source in our *Mixed* model is shown in … ... [9]

Authors 28/8/y 12:12
Formattato: Tipo di carattere:Corsivo

Authors 28/8/y 12:12
Eliminato: construction

Authors 28/8/y 12:12
Formattato: Tipo di carattere:Corsivo

Authors 28/8/y 12:12
Eliminato: a magnitude-frequency distribution

Authors 28/8/y 12:12
Formattato: Tipo di carattere:Corsivo

Authors 28/8/y 12:12
Eliminato: have been…modelled using ... [10]

three hazard curves overlap. Because the distance between Cesena and the closest fault sources is approximately 60 km, the impact of the fault input is less than the impact of the *distributed* source input. In this case, the choice of a particular MFD model has a limited impact on the modelling of *distributed* sources. Notably, for an annual frequency of exceedance (*AFOE*) lower than 10^{-4}, the *TGR fault* source input values are generally higher than those of the *CHG* source input, and the three models converge at *AFOE* < 10^{-4}. The resulting seismic hazard estimates depend on the assumed MFD model (*TGR* vs. *CHG*), especially for intermediate-magnitude events (5.5 to ~6.5). Because we assume that the maximum magnitude is imposed by the fault geometry and that the seismic moment release is controlled by the slip rate, the *TGR* model leads to the highest hazard values because this range of magnitude contributes the most to the hazard level.

In Figure 13, we investigated the influences of the Mixed *fault* source inputs and the Mixed *distributed* source inputs on the total hazard level of the entire study area, as well as the variability in the hazard results. The maps in Figure 13a show that the contribution of *fault* inputs to the total hazard level generally decreases as the exceedance probability increases from 2% to 81% in 50 years. At a 2% probability of exceedance in 50 years, the total hazard levels in the Apennines and eastern Sicily are mainly related to faults, whereas at an 81% probability of exceedance in 50 years, the contributions of *fault* inputs are high in local areas of central Italy and southern Calabria.

Moreover, we examined the contributions of *fault* and *distributed* sources along three E-W-oriented profiles in northern, central and southern Italy (Fig. 13b). Note that the contributions are not based on deaggregation but are computed according to the percentage of each source input in the AFOE value of the combined model. In areas with faults, the hazard level estimated by *fault* inputs is generally higher than that estimated by the corresponding *distributed* source inputs. Notable exceptions are present in areas proximal to slow-slipping active faults at an 81% probability of exceedance in 50 years (profile A), such as those at the eastern and western boundaries of the fault area in central Italy (profile B), and in areas where the contribution of the *distributed* source input is equal to that of the *fault* input at a 10% probability of exceedance in 50 years (eastern part of profile C).

Authors 28/8/y 12:12
Eliminato: model…is less than the imp ... [11]

Authors 28/8/y 12:12
Eliminato: 12… we investigated the inf ... [12]

Authors 28/8/y 12:12
Eliminato: the

Alessandro 28/8/y 14:48
Commenta [16]: After figure caption Fig. 12 by RC1.

Authors 28/8/y 12:12
Eliminato: 12b)….In areas with faults, ... [13]

Authors 28/8/y 12:12
Formattato: Tipo di carattere:Corsivo

Authors 28/8/y 12:12
Eliminato: model…is generally higher ... [14]

The features depicted by the three profiles result from a combination of the slip rates and spatial distributions of faults for *fault* source inputs. This pattern should be considered a critical aspect of using fault models for PSH analysis. In fact, the proposed approach requires a high level of expertise in active tectonics and cautious expert judgement at many levels in the procedure. First, the seismic hazard estimate is based on the definition of a segmentation model, which requires a series of rules based on observations and empirical regression between earthquakes and the size of the causative fault. New data might make it necessary to revise the rules or reconsider the role of the segmentation. In some cases, expert judgement could permit discrimination among different fault source models. Alternatively, all models should be considered branches in a logic tree approach.

Moreover, we propose a fault seismicity input in which the MFD of each fault source has been chosen based on an analysis of the occurrences of earthquakes that can be tentatively or confidently assigned to a certain fault. To describe the fault activity, we applied a probability density function to the magnitude, as commonly performed in the literature: the TGR model, where the maximum magnitude is the upper threshold and M_w = 5.5 is the lower threshold for all faults, and the characteristic maximum magnitude model, which consists of a truncated normal distribution centred on the maximum magnitude. Other MFDs have been proposed to model the earthquake recurrence of a fault. For example, Youngs and Coppersmith (1985) proposed a modification to the truncated exponential model to allow for the increased likelihood of characteristic events. However, we focused only on two models, as we believe that instead of a "blind" or qualitative characterization of the MFD of a fault source, future applications of statistical tests of the compatibility between expected earthquake rates and observed historical seismicity could be used as an objective method of identifying the optimal MFD of expected seismicity.

To focus on the general procedure for spatially integrating faults with sources representing distributed (or off-fault) seismicity, we did not investigate the impact of other smoothing procedures on the distributed sources, and we used fixed kernels with a constant bandwidth (as in the works of Kagan and Jackson, 1994; Frankel et al. 1997; Zechar and Jordan, 2010). The testing of adaptive bandwidths (e.g., Stock

Authors 28/8/y 12:12
Eliminato: in the
Authors 28/8/y 12:12
Eliminato: model
Authors 28/8/y 12:12
Eliminato: of
Authors 28/8/y 12:12
Eliminato: We finally
Authors 28/8/y 12:12
Eliminato: model
Authors 28/8/y 12:12
Eliminato: magnitude-frequency distribution
Authors 28/8/y 12:12
Eliminato: magnitude-frequency distributions
Authors 28/8/y 12:12
Eliminato: for
Authors 28/8/y 12:12
Eliminato: adjusting
Authors 28/8/y 12:12
Eliminato: ,
Authors 28/8/y 12:12
Eliminato: magnitude-frequency distribution
Authors 28/8/y 12:12
Eliminato: to
Authors 28/8/y 12:12
Eliminato: way to identify
Authors 28/8/y 12:12
Eliminato: best
Authors 28/8/y 12:12
Eliminato: magnitude-frequency distribution

and Smith, 2002; Helmstetter et al., 2006, 2007; Werner et al., 2011) or weighted combinations of both models has been reserved for future studies.

Finally, we compared, as shown in Figure 14, the 2013 European Seismic Hazard Model (ESHM13) developed within the SHARE project, the current Italian national seismic hazard map (MPS04) and the results of our model (Mixed model) using the same GMPEs as used in this study. Specifically, for ESHM13, we compared the results to the fault-based hazard map (FSBG model) that accounts for fault sources and background seismicity. The figure shows how the impact of our fault sources is more evident than in FSBG-ESHM13, and the comparison with MPS04 confirms a similar pattern, but with some significant differences at the regional to local scales.

The strength of our approach lies in the integration of different levels of information regarding the active faults in Italy, but the final result is unavoidably linked to the quality of the relevant data. Our work focused on presenting and applying a new approach for evaluating seismic hazards based on active faults and intentionally avoided the introduction of uncertainties due to the use of different segmentation rules or other slip rate values of faults. Moreover, the impact of ground motion predictive models is important in seismic hazard assessment but beyond the scope of this work. Future steps will be devoted to analysing these uncertainties and evaluating their impacts on seismic hazard estimates.

4. Conclusions

We presented our first national-scale PSH model of Italy, which summarizes and integrates the fault-based PSH models developed since the publication of Pace et al. in 2006.

The model proposed in this study combines fault source inputs based on over 110 faults grouped into 86 fault sources and distributed source inputs. For each fault source, the maximum magnitude and its uncertainty were derived by applying scaling relationships, and the rates of seismic activity were derived by applying slip rates to seismic moment evaluations and balancing these seismic moments using two MFD models.

Authors 28/8/y 12:12
Eliminato: implementations

Alessandro 28/8/y 14:50
Commenta [17]: After: Main Comment 2 and 3 by RC1 and General Comment number 3 by RC2.

Authors 28/8/y 12:12
Eliminato: is

Authors 28/8/y 12:12
Eliminato: possibility

Authors 28/8/y 12:12
Eliminato: integrating

Authors 28/8/y 12:12
Eliminato: on

Authors 28/8/y 12:12
Eliminato: databases

Authors 28/8/y 12:12
Eliminato: for

Authors 28/8/y 12:12
Eliminato: certainly

Authors 28/8/y 12:12
Eliminato: the

Authors 28/8/y 12:12
Eliminato: for

Authors 28/8/y 12:12
Eliminato: work

Authors 28/8/y 12:12
Eliminato: (

Authors 28/8/y 12:12
Eliminato:).

Authors 28/8/y 12:12
Eliminato: here

Authors 28/8/y 12:12
Eliminato: a

Authors 28/8/y 12:12
Eliminato: model

Authors 28/8/y 12:12
Eliminato: with

Authors 28/8/y 12:12
Eliminato: a

Authors 28/8/y 12:12
Eliminato: model

Authors 28/8/y 12:12
Eliminato: has been

Authors 28/8/y 12:12
Eliminato: have been

Authors 28/8/y 12:12
Eliminato: i

Authors 28/8/y 12:12
Eliminato: moment over

Authors 28/8/y 12:12
Eliminato: magnitude-frequency distributions

To account for unknown faults, a distributed seismicity input was applied following the well-known Frankel (1995) methodology to calculate seismicity parameters.

The fault sources and distributed sources have been integrated via a new approach based on the idea that deformation in the vicinity of an active fault is concentrated along the fault and that the seismic activity in the surrounding region is reduced. In particular, a distance-dependent linear weighting function has been introduced to allow the contribution of distributed sources (in the magnitude range overlapping the MFD of each fault source) to linearly decrease from 1 to 0 with decreasing distance from a fault. The strength of our approach lies in the ability to integrate different levels of available information for active faults that actually exist in Italy (or elsewhere), but the final result is unavoidably linked to the quality of the relevant data.

The PSH maps produced using our model show a hazard pattern similar to that of the current maps at the national scale, but some significant differences in hazard level are present at the regional to local scales (Figure 13).

Moreover, the impact that using different MFD models to derive seismic activity rates has on the hazard maps was investigated. The PGA values in the hazard maps generated by the *TGR* model are higher than those in the hazard maps generated by the *CHG* model. This difference is because the rates of earthquakes with magnitudes from 5.5 to approximately 6 are generally higher in the *TGR* model than in the *CHG* model. Moreover, the relative contributions of fault source inputs and distributed source inputs have been identified in maps and profiles in three sectors of the study area. These profiles show that the hazard level is generally higher where fault inputs are used, and for high probabilities of exceedance, the contribution of *distributed* inputs equals that of *fault* inputs.

Finally, the *Mixed* model was created by selecting the most appropriate MFD model for each fault. All data, including the locations and parameters of fault sources, are provided in the supplemental files of this paper.

This new PSH model is not intended to replace, integrate or assess the current official national seismic hazard model of Italy. While some aspects remain to be implemented in our approach (e.g., the integration of reverse/thrust faults in the database, sensitivity tests for the distance-dependent linear weighting function parameters, sensitivity tests for potential different segmentation models, and fault source inputs that account for fault interactions), the proposed model represents

Authors 28/8/y 12:12
Eliminato: model has also been…appli ... [15]

Authors 28/8/y 12:12
Eliminato: from the…distributed source ... [16]

Authors 28/8/y 12:12
Eliminato: probabilistic seismic hazard ... [17]

Authors 28/8/y 12:12
Eliminato: The…impact thaton the haz ... [18]

Authors 28/8/y 12:12
Eliminato: a preferred model, called ... [19]

Authors 28/8/y 12:12
Eliminato: test…the currently…official ... [20]

advancements in terms of input data (quantity and quality) and methodology based on a decade of research in the field of fault-based approaches to regional seismic hazard modelling.

Authors 28/8/y 12:12
Eliminato: an advance

References

Akinci, A., Galadini, F., Pantosti, D., Petersen, M., Malagnini, L., and Perkins, D.: Effect of Time Dependence on Probabilistic Seismic-Hazard Maps and Deaggregation for the Central Apennines, Italy, B Seismol Soc Am, 99, 585-610, 2009.

Akkar, S., Sandikkaya, M.A. , Bommer, J.J.: Empirical Ground-Motion Models for Point and Extended-Source Crustal Earthquake Scenarios in Europe and the Middle East, Bulletin of Earthquake Engineering, ISSN:1570-761X, 2013.

Basili, R., Valensise, G., Vannoli, P., Burrato, P., Fracassi, U., Mariano, S., Tiberti, M. M. and Boschi, E.: The Database of Individual Seismogenic Sources (DISS), version 3: Summarizing 20 years of research on Italy's earthquake geology, Tectonophysics, 453, 20- 43, 2008.

Benedetti, L., Manighetti, I., Gaudemer, Y., Finkel, R., Malavieille, J., Pou, K., Arnold, M., Aumaitre, G., Bourles, D., and Keddadouche, K.: Earthquake synchrony and clustering on Fucino faults (Central Italy) as revealed from in situ Cl-36 exposure dating, J Geophys Res-Sol Ea, 118, 4948-4974, 2013.

Bindi, D., Massa, M., Luzi, L., Ameri, G., Pacor, F., Puglia, R., and Augliera, P.: Pan-European ground-motion prediction equations for the average horizontal component of PGA, PGV, and 5%-damped PSA at spectral periods up to 3.0 s using the RESORCE dataset (vol 12, pg 391, 2014), B Earthq Eng, 12, 431-448, 2014.

Authors 28/8/y 12:12
Formattato: Tipo di carattere:Inglese (Regno Unito)

Authors 28/8/y 12:12
Formattato: Tipo di carattere:Inglese (Regno Unito)

Boncio, P., Brozzetti, F. and Lavecchia G.: Architecture and seismotectonics of a regional Low-Angle Normal Fault zone in Central Italy. Tectonics, 19 (6), 1038-1055, 2000.

Boncio, P., Lavecchia, G., and Pace, B.: Defining a model of 3D seismogenic sources for Seismic Hazard Assessment applications: The case of central Apennines (Italy), J Seismol, 8, 407-425, 2004.

Boncio, P., Pizzi, A., Cavuoto, G., Mancini, M., Piacentini, T., Miccadei, E., Cavinato, G. P., Piscitelli, S., Giocoli, A., Ferretti, G., De Ferrari, R., Gallipoli, M. R., Mucciarelli, M., Di Fiore, V., Franceschini, A., Pergalani, F., Naso, G., and Macroarea, W. G.: Geological and geophysical characterisation of the Paganica - San Gregorio area after the April 6, 2009 L'Aquila earthquake (M-w 6.3, central Italy): implications for site response, B Geofis Teor Appl, 52, 491-512, 2011.

Bull, J. M., Barnes, P. M., Lamarche, G., Sanderson, D. J., Cowie, P. A., Taylor, S. K., and Dix, J. K.: High-resolution record of displacement accumulation on an active normal fault: implications for models of slip accumulation during repeated earthquakes, J Struct Geol, 28, 1146-1166, 2006.

Chiou, B. S. J. and Youngs, R. R.: An NGA model for the average horizontal component of peak ground motion and response spectra, Earthq Spectra, 24, 173-215, 2008.

Cornell, C.A.: Engineering seismic risk analysis, Bull. Seism. Soc. Am., 58,1583-1606, 1968.

Cowie, P. A.: A healing-reloading feedback control on the growth rate of seismogenic faults, J Struct Geol, 20, 1075-1087, 1998.

Cowie, P. A., Roberts, G. P., Bull, J. M., and Visini, F.: Relationships between fault geometry, slip rate variability and earthquake recurrence in extensional settings, Geophys J Int, 189, 143-160, 2012.

Cowie, P. A., Underhill, J. R., Behn, M. D., Lin, J., and Gill, C. E.: Spatio-temporal evolution of strain accumulation derived from multi-scale observations of Late Jurassic rifting in the northern North Sea: A critical test of models for lithospheric extension, Earth Planet Sc Lett, 234, 401-419, 2005.

Authors 28/8/y 12:12
Formattato: Tipo di carattere:Inglese (Regno Unito)

Authors 28/8/y 12:12
Eliminato: '

Authors 28/8/y 12:12
Formattato: Tipo di carattere:Inglese (Regno Unito)

Cowie, P. A., Vanneste, C., and Sornette, D.: Statistical Physics Model for the Spatiotemporal Evolution of Faults, J Geophys Res-Sol Ea, 98, 21809-21821, 1993.

D'amato, D., Pace, B., Di Nicola, L., Stuart, F.M., Visini, F., Azzaro, R., Branca, S., and Barfod, D.N.: Holocene slip rate variability along the Pernicana fault system (Mt. Etna, Italy): Evidence from offset lava flows: GSA Bulletin, doi:10.1130/B31510.1, 2016.

Faccioli, E., Bianchini, A., and Villani, M.: New ground motion prediction equations for t > 1 s and their influence on seismic hazard assessment, In: Proceedings of the University of Tokyo symposium on long-period ground motion and urban disaster mitigation, 2010.

Ferranti, L., Palano, M., Cannavo, F., Mazzella, M. E., Oldow, J. S., Gueguen, E., Mattia, M., and Monaco, C.: Rates of geodetic deformation across active faults in southern Italy, Tectonophysics, 621, 101-122, 2014.

Field, E. H., Biasi, G. P., Bird, P., Dawson, T. E., Felzer, K. R., Jackson, D. D., Johnson, K. M., Jordan, T. H., Madden, C., Michael, A. J., Milner, K. R., Page, M. T., Parsons, T., Powers, P. M., Shaw, B. E., Thatcher, W. R., Weldon, R. J., and Zeng, Y. H.: Long-Term Time-Dependent Probabilities for the Third Uniform California Earthquake Rupture Forecast (UCERF3), B Seismol Soc Am, 105, 511-543, 2015.

Field, E. H., Jackson, D. D., and Dolan, J. F.: A mutually consistent seismic-hazard source model for southern California, B Seismol Soc Am, 89, 559-578, 1999.

Finnegan, N. J., Schumer, R., and Finnegan, S.: A signature of transience in bedrock river incision rates over timescales of 10(4)-10(7) years, Nature, 505, 391-+, 2014.

Frankel, A.: Simulating Strong Motions of Large Earthquakes Using Recordings of Small Earthquakes - the Loma-Prieta Mainshock as a Test-Case, B Seismol Soc Am, 85, 1144-1160, 1995.

Frankel, A., Mueller, C., Barnhard, T., Perkins, D., Leyendecker, E. V., Dickman, N., Hanson, S.. and Hopper, M.: Seismic-hazard maps for California, Nevada, and Western Arizona/Utah', U.S. Geological Survey Open-File Rept. 97-130, 1997.

Authors 28/8/y 12:12
Formattato: Tipo di carattere:Inglese (Regno Unito)

Authors 28/8/y 12:12
Eliminato: '

Authors 28/8/y 12:12
Formattato: Tipo di carattere:Inglese (Regno Unito)

Gallen, S. F., Pazzaglia, F. J., Wegmann, K. W., Pederson, J. L., and Gardner, T. W.: The dynamic reference frame of rivers and apparent transience in incision rates, Geology, 43, 623-626, 2015.

Garcia-Mayordomo, J., Gaspar-Escribano, J. M., and Benito, B.: Seismic hazard assessment of the Province of Murcia (SE Spain): analysis of source contribution to hazard, J Seismol, 11, 453-471, 2007.

Gardner, J. K., Knopoff, L.: Is the sequence of earthquakes in Southern California, with aftershocks removed, Poissonian?', Bulletin of the Seismological Society of America, 64, 1363-1367, 1974.

Gardner, T. W., Jorgensen, D. W., Shuman, C., and Lemieux, C. R.: Geomorphic and Tectonic Process Rates - Effects of Measured Time Interval, Geology, 15, 259-261, 1987.

Gasperini P., Bernardini F., Valensise G. and Boschi E.: Defining Seismogenic Sources from Historical Earthquake Felt Reports, *Bull. Seism. Soc. Am.*, 89, 94-110, 1999.

GEM: The OpenQuake-engine User Manual. Global Earthquake Model (GEM) Technical Report, doi: 10.13117/GEM.OPENQUAKE.MAN.ENGINE.1.9/01, 189 pages, 2016.

Gunderson, K. L., Anastasio, D. J., Pazzaglia, F. J., and Picotti, V.: Fault slip rate variability on 10(4)-10(5)yr timescales for the Salsomaggiore blind thrust fault, Northern Apennines, Italy, Tectonophysics, 608, 356-365, 2013.

Hanks, T. C., and Kanamori, H.: A moment magnitude scale, Journal of Geophysics Research, 84, 2348–2350, 1979.

Helmstetter, A., Kagan, Y. Y., and Jackson, D. D.: Comparison of short-term and time-independent earthquake forecast models for southern California, B Seismol Soc Am, 96, 90-106, 2006.

Helmstetter, A., Kagan, Y. Y., and Jackson, D. D.: High-resolution time-independent grid-based forecast for M <= 5 earthquakes in California, Seismol Res Lett, 78, 78-86, 2007.

International Association of Seismology and Physics of the Earth's Interior (IASPEI): Summary of Magnitude Working Group recommendations on standard procedures for determining earthquake magnitudes from digital data, http://www.iaspei.org/

Authors 28/8/y 12:12
Eliminato: '

Authors 28/8/y 12:12
Formattato: Tipo di carattere:Inglese (Regno Unito)

Authors 28/8/y 12:12
Formattato: Tipo di carattere:Inglese (Regno Unito)

commissions/CSOI/summary_of_WG_recommendations_2005.pdf (last accessed December 2015), 2005.
Kagan, Y. Y.: Seismic moment distribution revisited: I. Statistical results, Geophys J Int, 148, 520-541, 2002.
Kagan, Y., and Knopoff, L.: Earthquake risk prediction as a stochastic process, Physics of the Earth and Planetary Interiors, 14, 97–108, 1977.
Kagan, Y. Y. and Jackson, D. D.: Long-Term Probabilistic Forecasting of Earthquakes, J Geophys Res-Sol Ea, 99, 13685-13700, 1994.
Kamer, Y. and Hiemer, S.: Data-driven spatial b value estimation with applications to California seismicity: To b or not to b, J Geophys Res-Sol Ea, 120, 5191-5214, 2015.
King, G. C. P., Stein, R. S., and Lin, J.: Static Stress Changes and the Triggering of Earthquakes, B Seismol Soc Am, 84, 935-953, 1994.
Kostrov, V. V.: Seismic moment and energy of earthquakes, and seismic flow of rock, Physic of the Solid Earth, 1, 23-44, 1974.
Leonard, M.: Earthquake fault scaling: Self-consistent relating of rupture length, width, average displacement, and moment release. Bulletin of the Seismological Society of America, 100(5A), 1971- 1988, 2010.
Machette, M.N.: Active, capable, and potentially active faults; a paleoseismic perspective, J. Geodyn., 29, 387–392, 2000.
Main, I.: Statistical physics, seismogenesis, and seismic hazard, Rev Geophys, 34, 433-462, 1996.
Mansfield, C. and Cartwright, J.: Fault growth by linkage: observations and implications from analogue models, J Struct Geol, 23, 745-763, 2001.
Meletti, C., Visini, F., D'Amico, V., and Rovida A.: Seismic hazard in central Italy and the 2016 Amatrice earthquake, Annals of Geophysics, 59, doi:10.4401/ag-7248, 2016.
McClymont, A. F., Villamor, P., and Green, A. G.: Assessing the contribution of off-fault deformation to slip-rate estimates within the Taupo Rift, New Zealand, using 3-D ground-penetrating radar surveying and trenching, Terra Nova, 21, 446-451, 2009a.
McClymont, A. F., Villamor, P., and Green, A. G.: Fault displacement accumulation and slip rate variability within the Taupo Rift (New Zealand) based on trench and 3-D ground-penetrating radar data, Tectonics, 28, 2009b.

Authors 28/8/y 12:12
Formattato: Tipo di carattere:Inglese (Regno Unito)

Authors 28/8/y 12:12
Eliminato: '

Authors 28/8/y 12:12
Formattato: Tipo di carattere:Inglese (Regno Unito)

Nicol, A., Walsh, J., Berryman, K., and Villamor, P.: Interdependence of fault displacement rates and paleoearthquakes in an active rift, Geology, 34, 865-868, 2006.

Nicol, A., Walsh, J., Mouslopoulou, V., and Villamor, P.: Earthquake histories and Holocene acceleration of fault displacement rates, Geology, 37, 911-914, 2009.

Nicol, A., Walsh, J. J., Villamor, P., Seebeck, H., and Berryman, K. R.: Normal fault interactions, paleoearthquakes and growth in an active rift, J Struct Geol, 32, 1101-1113, 2010.

Nicol, A., Walsh, J. J., Watterson, J., and Underhill, J. R.: Displacement rates of normal faults, Nature, 390, 157-159, 1997.

Ordaz, M. and Reyes, C.: Earthquake hazard in Mexico City: Observations versus computations, B Seismol Soc Am, 89, 1379-1383, 1999.

Pace, B., Bocchini, G. M., and Boncio, P.: Do static stress changes of a moderate-magnitude earthquake significantly modify the regional seismic hazard? Hints from the L'Aquila 2009 normal-faulting earthquake (Mw 6.3, central Italy), Terra Nova, 26, 430-439, 2014.

Pace, B., Peruzza, L., Lavecchia, G., and Boncio, P.: Layered seismogenic source model and probabilistic seismic-hazard analyses in central Italy, B Seismol Soc Am, 96, 107-132, 2006.

Pace, B., Visini, F., and Peruzza, L.: FiSH: MATLAB Tools to Turn Fault Data into Seismic-Hazard Models, Seismol Res Lett, 87, 374-386, 2016.

Peruzza, L., and Pace B.: Sensitivity analysis for seismic source characteristics to probabilistic seismic hazard assessment in central Apennines (Abruzzo area), Bollettino di Geofisica Teorica ed Applicata 43, 79–100, 2002.

Peruzza, L., Pace, B., and Visini, F.: Fault-Based Earthquake Rupture Forecast in Central Italy: Remarks after the L'Aquila M-w 6.3 Event, B Seismol Soc Am, 101, 404-412, 2011.

Peruzza, L., Gee, R., Pace, B., Roberts, G., Scotti, O., Visini,F., Benedetti, L., and Pagani, M.: PSHA after a strong earthquake: hints for the recovery, Annals of Geophysics, 59, doi:10.4401/ag-7257, 2016

Roberts, G. P., Cowie, P., Papanikolaou, I., and Michetti, A. M.: Fault scaling relationships, deformation rates and seismic hazards: an example from the Lazio-Abruzzo Apennines, central Italy, J Struct Geol, 26, 377-398, 2004.

Authors 28/8/y 12:12
Eliminato: '

Authors 28/8/y 12:12
Formattato: Tipo di carattere:Inglese (Regno Unito)

Authors 28/8/y 12:12
Eliminato: '

Authors 28/8/y 12:12
Formattato: Tipo di carattere:Inglese (Regno Unito)

Roberts, G. P. and Michetti, A. M.: Spatial and temporal variations in growth rates along active normal fault systems: an example from The Lazio-Abruzzo Apennines, central Italy, J Struct Geol, 26, 339-376, 2004.

Robinson, R., Nicol, A., Walsh, J. J., and Villamor, P.: Features of earthquake occurrence in a complex normal fault network: Results from a synthetic seismicity model of the Taupo Rift, New Zealand, J Geophys Res-Sol Ea, 114, 2009.

Rovida, A., Locati, M., Camassi, R., Lolli, B., and Gasperini P.: CPTI15, the 2015 version of the Parametric Catalogue of Italian Earthquakes. Istituto Nazionale di Geofisica e Vulcanologia. doi:http://doi.org/10.6092/INGV.IT-CPTI15, 2016.

Scotti, O., Clement, C., and Baumont, D.: Seismic hazard for design and verification of nuclear installations in France: regulatory context, debated issues and ongoing developments, B Geofis Teor Appl, 55, 135-148, 2014.

Stein, R. S., King, G. C. P., and Lin, J.: Stress Triggering of the 1994 M=6.7 Northridge, California, Earthquake by Its Predecessors, Science, 265, 1432-1435, 1994.

Stirling, M., McVerry, G., Gerstenberger, M., Litchfield, N., Van Dissen, R., Berryman, K., Barnes, P., Wallace, L., Villamor, P., Langridge, R., Lamarche, G., Nodder, S., Reyners, M., Bradley, B., Rhoades, D., Smith, W., Nicol, A., Pettinga, J., Clark, K., and Jacobs, K.: National Seismic Hazard Model for New Zealand: 2010 Update, B Seismol Soc Am, 102, 1514-1542, 2012.

Stock, C. and Smith, E. G. C.: Adaptive kernel estimation and continuous probability representation of historical earthquake catalogs, B Seismol Soc Am, 92, 904-912, 2002a.

Stock, C. and Smith, E. G. C.: Comparison of seismicity models generated by different kernel estimations, B Seismol Soc Am, 92, 913-922, 2002b.

Stucchi, M., Meletti, C., Montaldo, V., Crowley, H., Calvi, G. M., and Boschi, E.: Seismic Hazard Assessment (2003-2009) for the Italian Building Code, B Seismol Soc Am, 101, 1885-1911, 2011.

Verdecchia, A. and Carena, S.: Coulomb stress evolution in a diffuse plate boundary: 1400 years of earthquakes in eastern California and western Nevada, USA, Tectonics, 35, 1793-1811, 2016.

Visini, F. and Pace, B.: Insights on a Key Parameter of Earthquake Forecasting, the Coefficient of Variation of the Recurrence Time, Using a Simple Earthquake Simulator, Seismol Res Lett, 85, 703-713, 2014.

Weichert, D. H: Estimation of the earthquake recurrence parameters for unequal observation periods for different magnitudes, Bulletin of the Seismological Society of America, 70, 1337-1346, 1980.

Wells, D. L. and Coppersmith, K. J.: New Empirical Relationships among Magnitude, Rupture Length, Rupture Width, Rupture Area, and Surface Displacement, B Seismol Soc Am, 84, 974-1002, 1994.

Werner, M. J., Helmstetter, A., Jackson, D. D., Kagan, Y. Y., and Wiemer, S.: Adaptively smoothed seismicity earthquake forecasts for Italy, Ann Geophys-Italy, 53, 107-116, 2010.

Woessner, J., Laurentiu, D., Giardini, D., Crowley, H., Cotton, F., Grunthal, G., Valensise, G., Arvidsson, R., Basili, R., Demircioglu, M. B., Hiemer, S., Meletti, C., Musson, R. W., Rovida, A. N., Sesetyan, K., Stucchi, M., and Consortium, S.: The 2013 European Seismic Hazard Model: key components and results, B Earthq Eng, 13, 3553-3596, 2015.

Youngs, R. R. and Coppersmith, K. J.: Implications of Fault Slip Rates and Earthquake Recurrence Models to Probabilistic Seismic Hazard Estimates, B Seismol Soc Am, 75, 939-964, 1985.

Zechar, J. D. and Jordan, T. H.: Simple smoothed seismicity earthquake forecasts for Italy, Ann Geophys-Italy, 53, 99-105, 2010.

Zhao, J. X., Zhang, J., Asano, A., Ohno, Y., Oouchi, T., Takahashi, T., Ogawa, H., Irikura, K., Thio, H. K., Somerville, P. G., Fukushima, Y., and Fukushima, Y.: Attenuation relations of strong ground motion in Japan using site classification based on predominant period, B Seismol Soc Am, 96, 898-913, 2006.

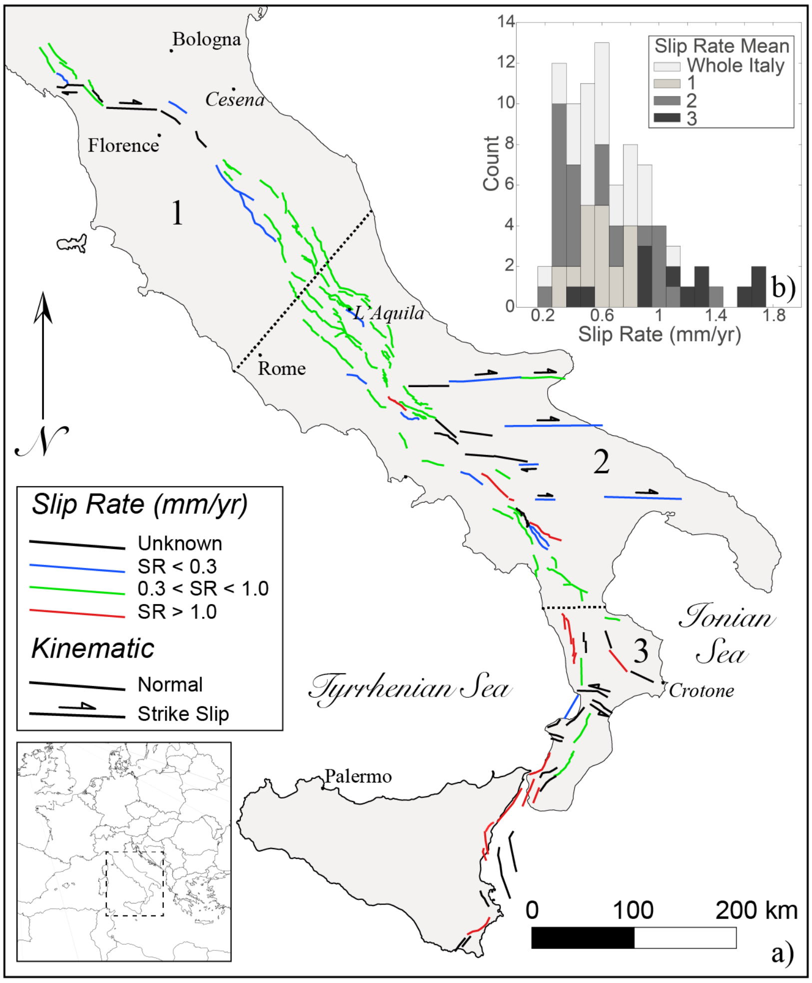

Fig. 1 a) Map of normal and strike-slip active faults used in this study. The colour scale indicates the slip rate. b) Histogram of the slip rate distribution in the entire study area and in three subsectors. The numbers 1, 2 and 3 represent the Northern Apennines, Central-Southern Apennines and Calabria-Sicilian coast regions, respectively. The dotted black lines are the boundaries of the regions.

Authors 28/8/y 12:12
Eliminato: Colour

Authors 28/8/y 12:12
Eliminato: for

Authors 28/8/y 12:12
Eliminato: whole

Authors 28/8/y 12:12
Eliminato: for

Authors 28/8/y 12:12
Eliminato: sub-sectors

Authors 28/8/y 12:12
Eliminato: are for

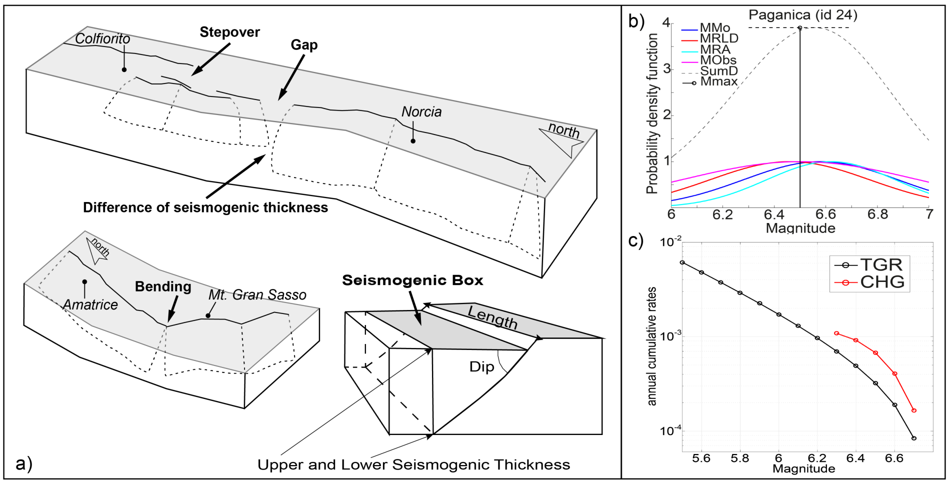

Fig. 2 a) Conceptual model of active faults and segmentation rules adopted to define a fault source and its planar projection, forming a seismogenic box [modified from Boncio et al., 2004]. b) Example of FiSH code output (see Pace et al., 2016 for details) for the Paganica fault source showing the magnitude estimates from empirical relationships and observations, both of which are affected by uncertainties. In this example, four magnitudes are estimated: MMo (blue line) is from the standard formula (IASPEI, 2005); MRLD (red line) and MRA (cyan line) correspond to estimates based on the maximum subsurface fault length and maximum rupture area from the empirical relationships of Wells and Coppersmith (1994) for length and area, respectively; and Mobs (magenta line) is the largest observed moment magnitude. The black dashed line represents the summed probability density curve (SumD), the vertical black line represents the central value of the Gaussian fit of the summed probability density curve (Mmax), and the horizontal black dashed line represents its standard deviation (σMmax). The input values that were used to obtain this output are provided in Table 1. c) Comparison of the magnitude–frequency distributions of the Paganica source, which were obtained using the CHG model (red line) and the TGR model (black line).

Authors 28/8/y 12:12
Eliminato: by

Authors 28/8/y 12:12
Formattato: Tipo di carattere:Inglese (Regno Unito)

Authors 28/8/y 12:12
Eliminato: ,

Authors 28/8/y 12:12
Eliminato: combination of

Authors 28/8/y 12:12
Eliminato: (MRLD, red line)

Authors 28/8/y 12:12
Eliminato: (MRA, cyan line) are

Authors 28/8/y 12:12
Eliminato: for

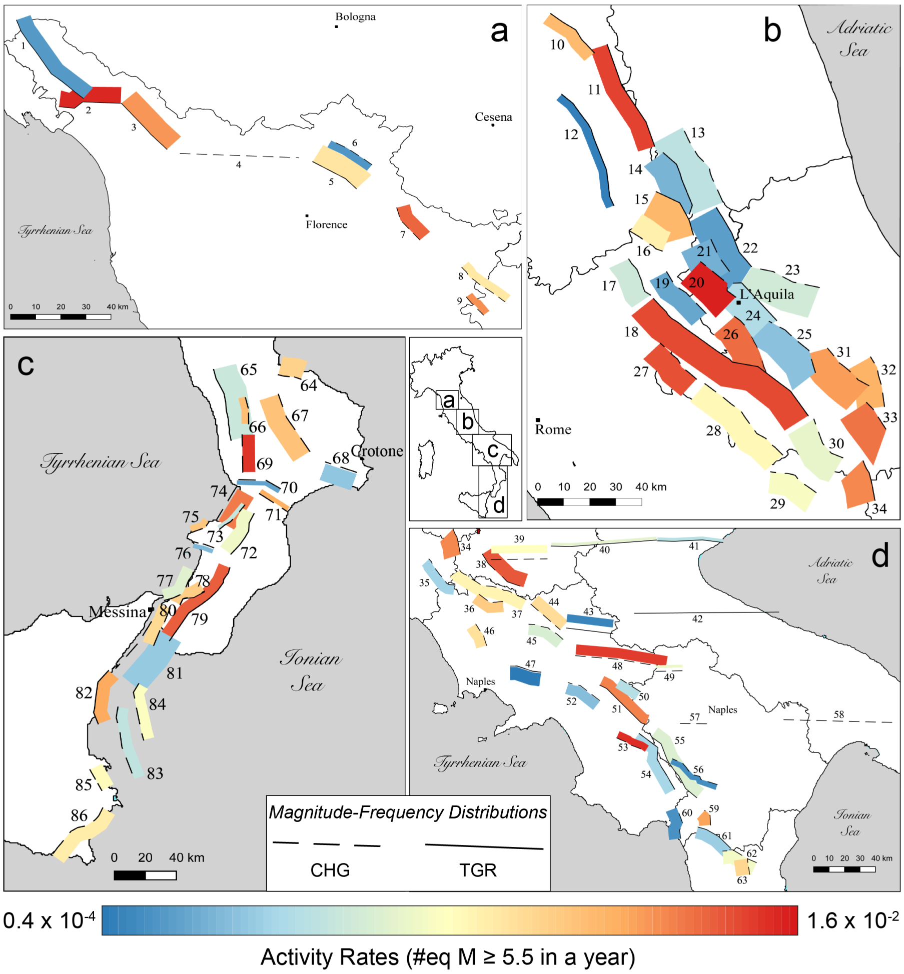

Fig. 3 Maps showing the fault source inputs as seismogenic boxes (see Fig. 2a). The colour scale indicates the activity rate. Solid and dashed lines (corresponding to the uppermost edge of the fault) are used to highlight our choice between the two end-members of the MFD model adopted in the so-called *Mixed* model.

Unknown
Formattato: Tipo di carattere:12 pt

Authors 28/8/y 12:12

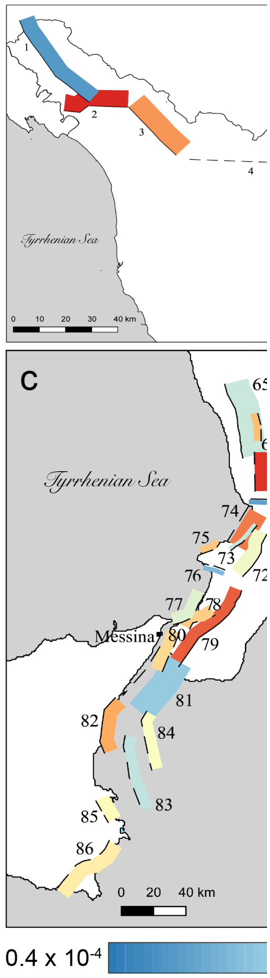

Eliminato:

Authors 28/8/y 12:12
Eliminato: model

Unknown
Formattato: Tipo di carattere:12 pt

Authors 28/8/y 12:12
Eliminato: Colour

Authors 28/8/y 12:12
Eliminato: in correspondence of

Authors 28/8/y 12:12
Eliminato: magnitude-frequency distributions

Authors 28/8/y 12:12
Eliminato: here for

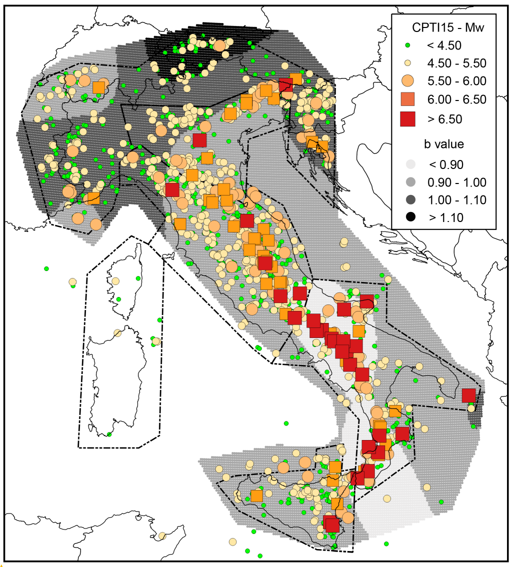

Fig. 4 Historical earthquakes from the most recent version of the historical parametric Italian catalogue (CPTI15, Rovida et al., 2016), the spatial variations in b-values and the polygons defining the five macroseismic areas used to assess the magnitude intervals.

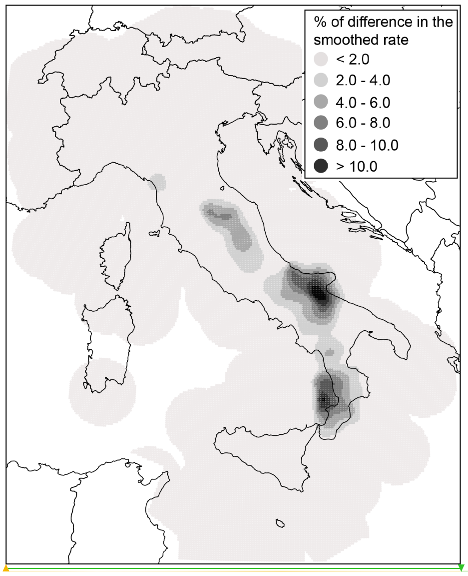

Fig. 5 Differences in percentages between the two smoothed rates produced by eq. (2) using the complete catalogue and the modified catalogue without events associated with known active faults (*TGR* model)

Alessandro 28/8/y 14:52
Eliminato:

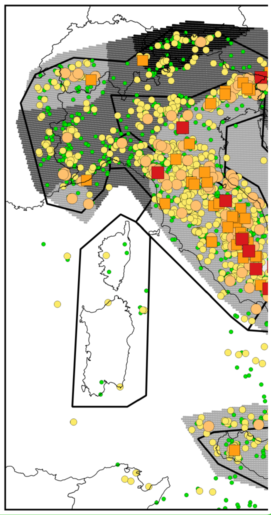

Unknown
Formattato: Tipo di carattere:12 pt

Authors 28/8/y 12:12
Eliminato: completeness

Unknown
Formattato: Tipo di carattere:12 pt

Alessandro 28/8/y 14:53
Eliminato:

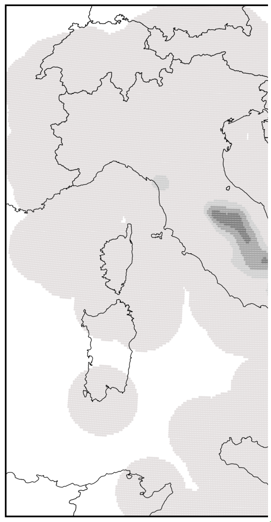

Authors 28/8/y 12:12
Eliminato: 1

Authors 28/8/y 12:12
Eliminato:).

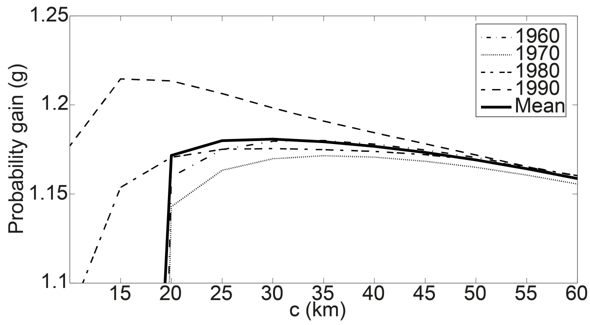

Fig. 6 Probability gain per earthquake (see eq. 3) versus correlation distance *c*, highlighting the best radius for use in the smoothed seismicity approach (eq. 2).

Authors 28/8/y 12:12
Eliminato: 2

Authors 28/8/y 12:12
Formattato: Tipo di carattere:Corsivo

Authors 28/8/y 12:12
Eliminato: showing

Authors 28/8/y 12:12
Eliminato: 1).

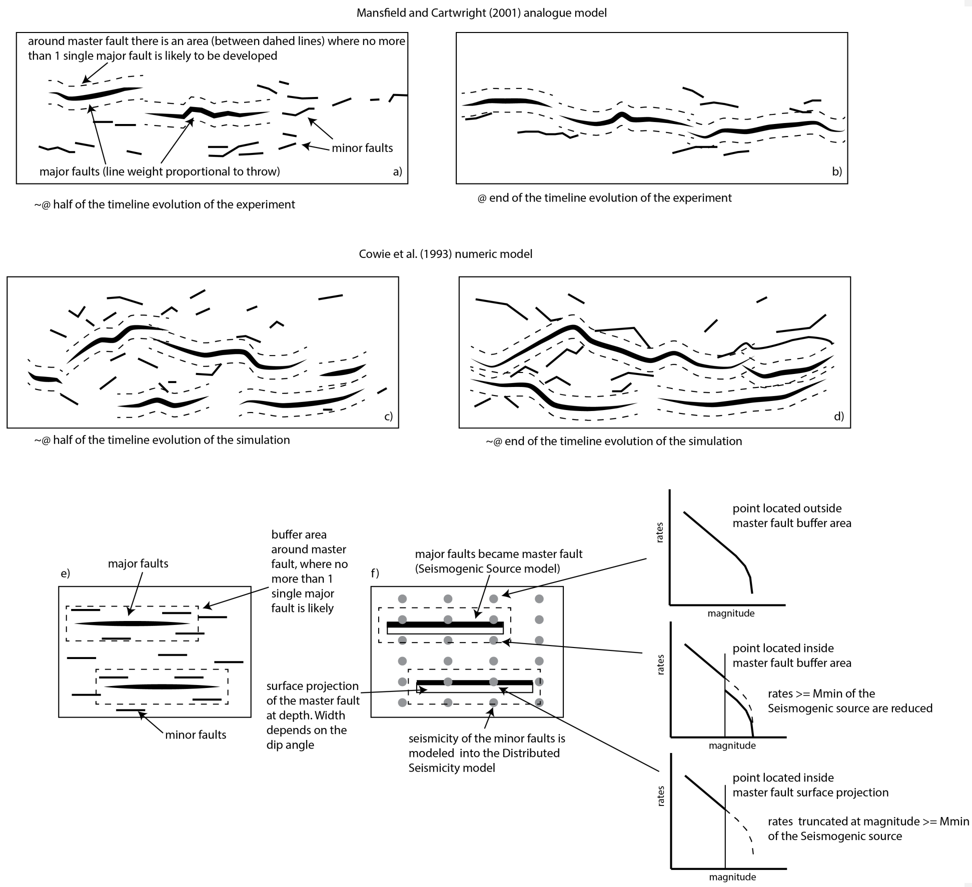

Fig. 7 Fault system evolution and implications in our model. a) and b) Diagrams from the Mansfield and Cartwright (2001) analogue experiment in two different stages: the approximate midpoint of the sequence and the end of the sequence. Areas exist around master faults where no more than a single major fault is likely to develop. c) and d) Diagrams from numerical modelling conducted by Cowie et al. (1993) in two different stages. This experiment shows the similar evolutional features of major and minor faults. e) and f) Application of the analogue and numerical modelling of fault system evolution to the fault source input proposed in this paper. A buffer area is drawn around each fault source, where it is unlikely for other major faults to develop, and it accounts for the length and slip rate of the fault source. This buffer area is useful for reducing or truncating the rates of expected distributed seismicity based on the position of a distributed seismicity point with respect to the buffer zone (see the text for details).

Authors 28/8/y 12:12
Eliminato: Sketches

Authors 28/8/y 12:12
Eliminato: at

Authors 28/8/y 12:12
Eliminato: approximately

Authors 28/8/y 12:12
Eliminato: Around

Authors 28/8/y 12:12
Eliminato: , there is an area

Authors 28/8/y 12:12
Eliminato: Sketches

Authors 28/8/y 12:12
Eliminato: at

Authors 28/8/y 12:12
Eliminato: model

Authors 28/8/y 12:12
Eliminato: taking into account

Authors 28/8/y 12:12
Eliminato: seismicity of the

Authors 28/8/y 12:12
Eliminato: , depending

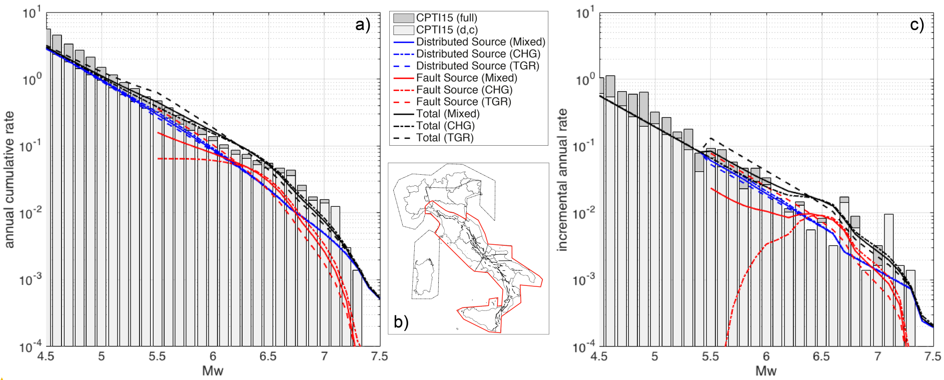

Fig. 8 a) annual cumulative rate and c) incremental annual rate computed for the red bounded area in b). The rates have been computed using: (i) the full CPTI15 catalogue; (ii) the declustered and complete catalogue (CPTI15 (d, c) in the legend) obtained using the completeness magnitude thresholds over different periods of time given by Stucchi et al. (2011) for five large zones; (iii) the distributed sources; (iv) the fault sources; and (v) summing fault and distributed sources (Total).

Unknown
Formattato: Tipo di carattere:12 pt

Alessandro 28/8/y 14:54
Commenta [18]: After: Main Comment number 4 and Detailed Comment L409-411 by RC1; and General Comments 12 and 13 by RC2.

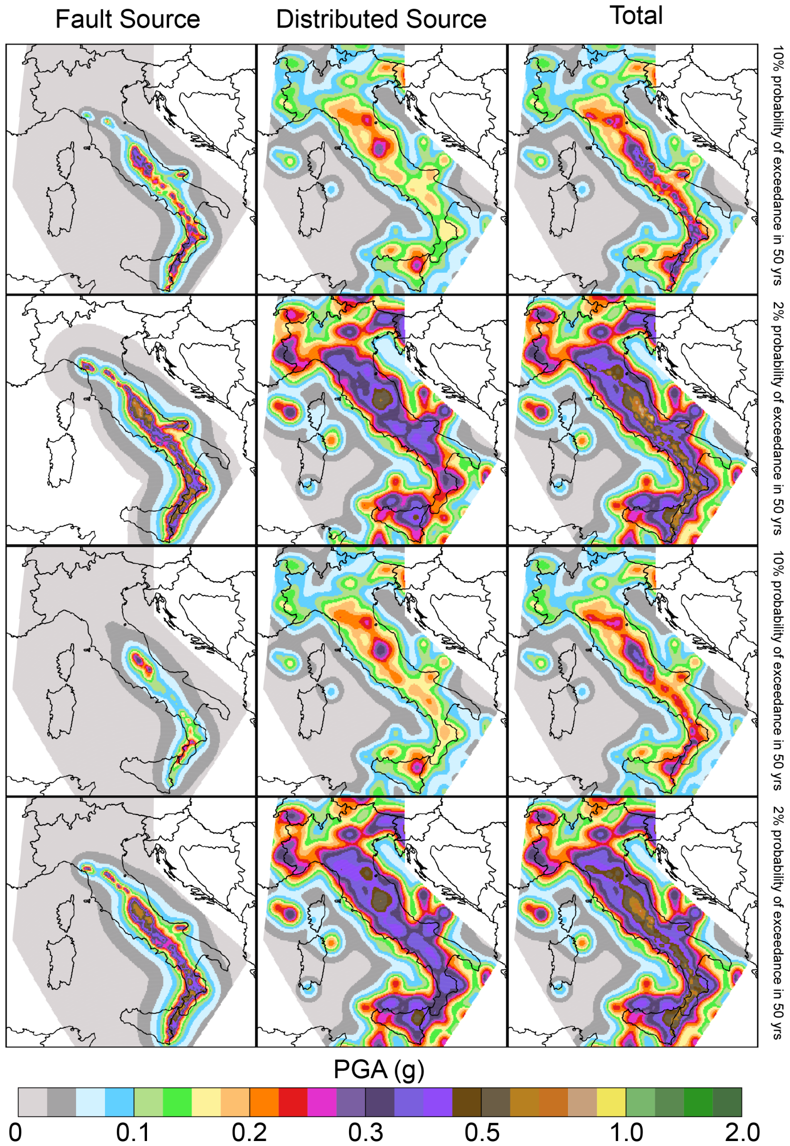

Fig. 9 Seismic hazard maps for the *TGR* and *CHG* models expressed in terms of peak ground acceleration (PGA) and computed for a latitude/longitude grid spacing of 0.05°. The first and second rows show the fault source, distributed source and total maps of the *TGR* model computed for 10% probability of exceedance in 50 years and 2% probability of exceedance in 50 years, corresponding to return periods of 475 and 2475 years, respectively. The third and fourth rows show the same maps for the *CHG* model.

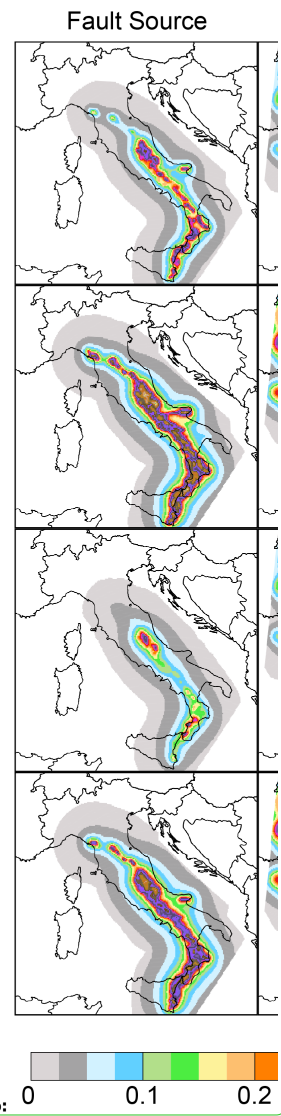

Eliminato:

Unknown

Formattato: Tipo di carattere:12 pt

Authors 28/8/y 12:12

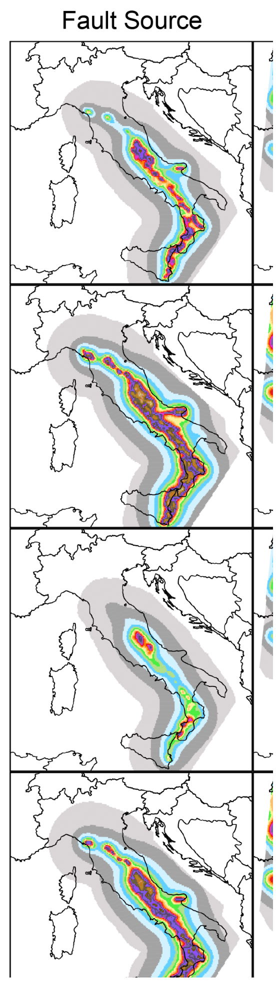

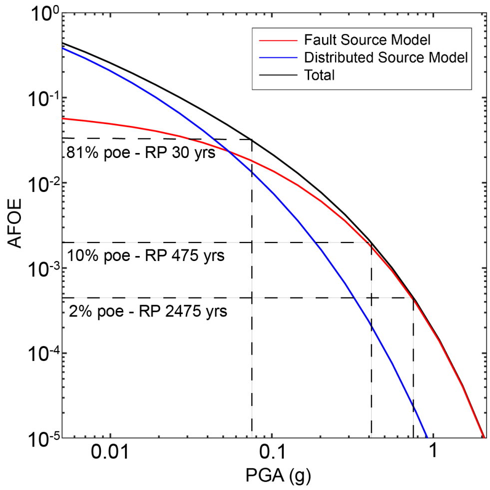

Fig. 10 An example of the contribution to the total seismic hazard level (black line), in terms of hazard curves, by the *fault* (red line) and *distributed* (blue line) source inputs for one of the 45,602 grid points (L'Aquila, 42.400-13.400). The dashed lines represent the 2%, 10% and 81% probabilities of exceedance (poes) in 50 years.

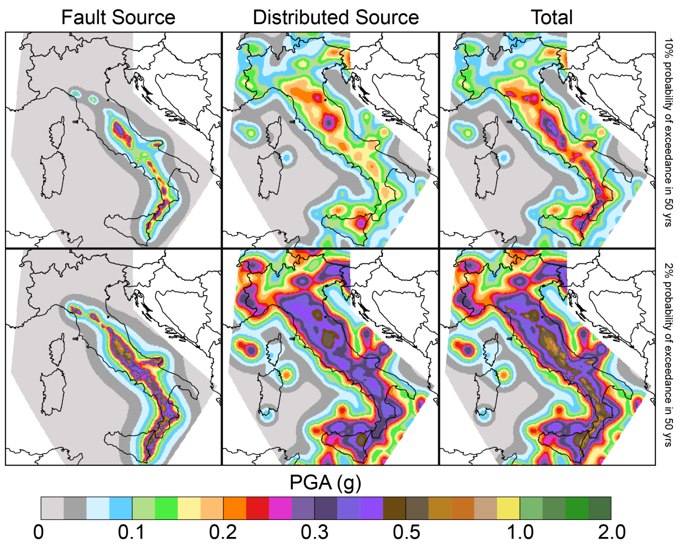

Fig. 11 Seismic hazard maps for the *Mixed* model. The first row shows the fault source, distributed source and total maps computed for 10% probability of

Authors 28/8/y 12:12
Eliminato: 9

Authors 28/8/y 12:12
Eliminato: models

Alessandro 28/8/y 14:55
Eliminato:

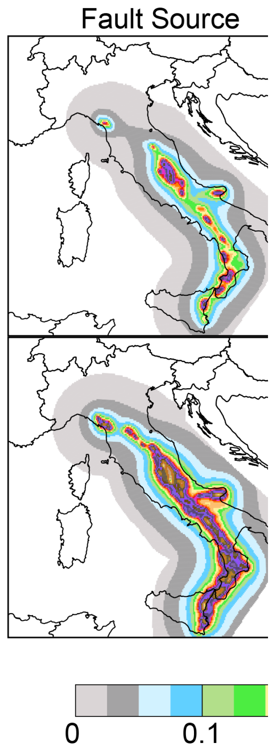

Unknown
Formattato: Tipo di carattere:12 pt

Authors 28/8/y 12:12
Eliminato: 10

Authors 28/8/y 12:12
Eliminato: Fault Source, Distributed Source

Authors 28/8/y 12:12
Eliminato: T

exceedance in 50 years, and the second row shows the same maps but computed for 2% probability of exceedance in 50 years, corresponding to return periods of 475 and 2475 years, respectively. The results are expressed in terms of peak ground acceleration (PGA).

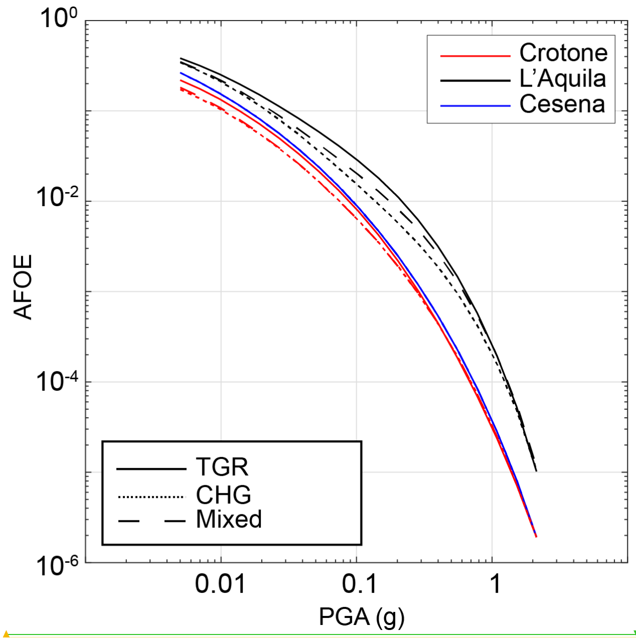

Fig. 12 *CHG* (dotted line), *TGR* (solid line) and *Mixed* model (dashed line) hazard curves for three sites: Cesena (red line), L'Aquila (black line) and Crotone (blue line)

Unknown
Formattato: Tipo di carattere:12 pt

Alessandro 28/8/y 14:59

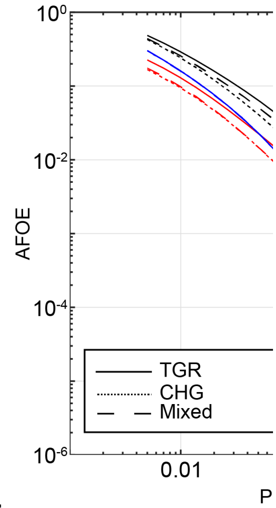

Eliminato:

Authors 28/8/y 12:12
Eliminato: 11

Authors 28/8/y 12:12
Eliminato:).

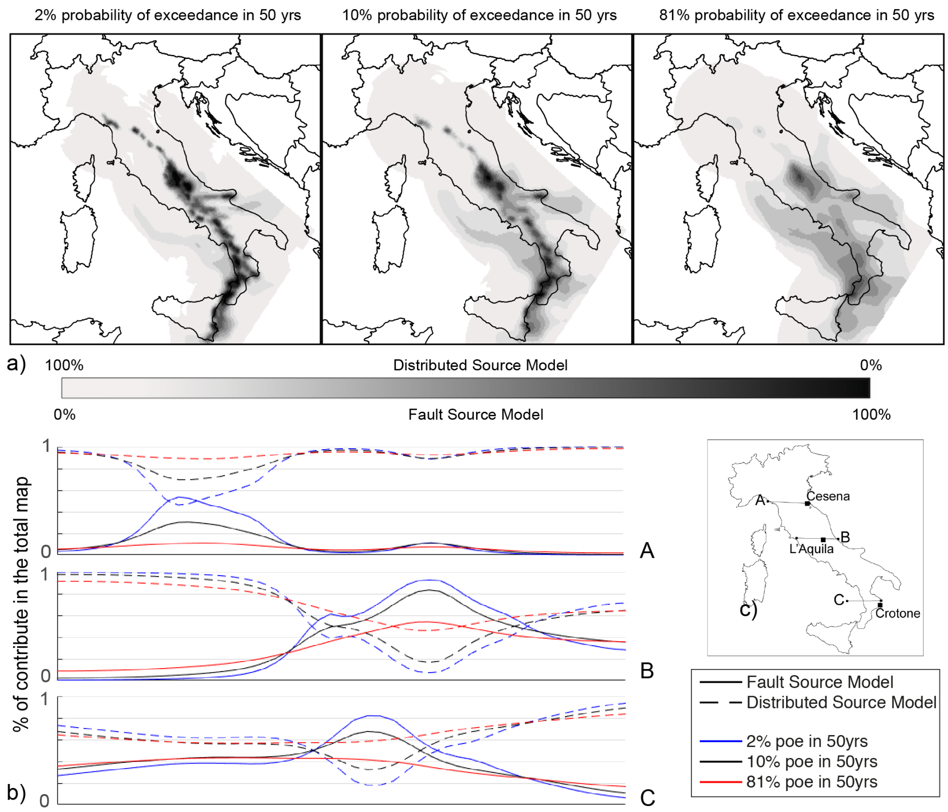

Fig. 13 a) Contribution maps of the Mixed *fault* and *distributed* source inputs to the total hazard level for three probabilities of exceedance: 2%, 10% and 81%, corresponding to return periods of 2475, 475 and 30 years, respectively. b) Contributions of the Mixed *fault* (solid line) and *distributed* (dashed line) source inputs along three profiles (A, B and C in Fig. 13c) for three probabilities of exceedance: 2% (blue line), 10% (black line) and 81% (red line).

Unknown
Formattato: Tipo di carattere:12 pt

Alessandro 28/8/y 14:59

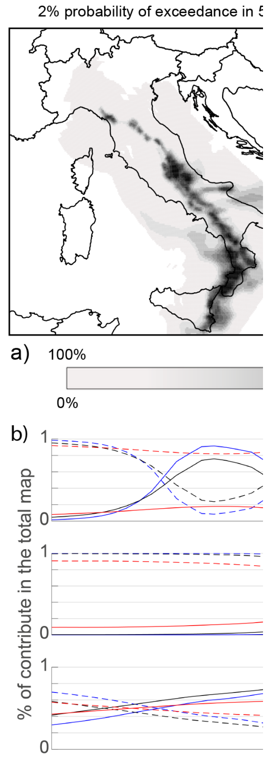

Eliminato:

Authors 28/8/y 12:12
Eliminato: 12

Authors 28/8/y 12:12
Eliminato: source model

Authors 28/8/y 12:12
Eliminato: Mixed

Authors 28/8/y 12:12
Eliminato: model

Authors 28/8/y 12:12
Eliminato: Mixed

Authors 28/8/y 12:12
Eliminato: models

Authors 28/8/y 12:12
Eliminato: 2

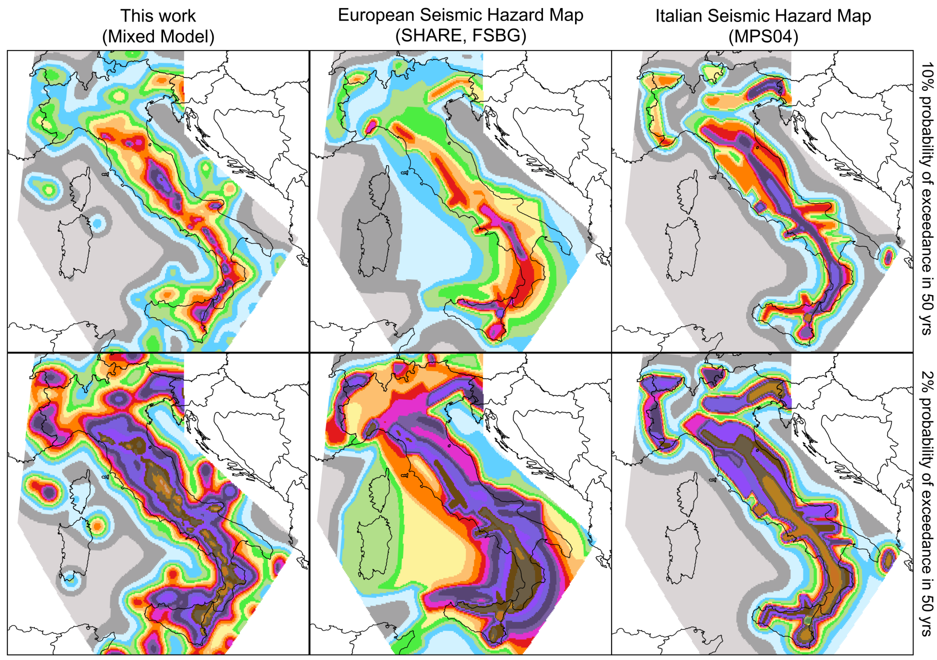

Fig. 14 Seismic hazard maps expressed in terms of Peak Ground Acceleration (PGA) and computed for a latitude/longitude grid spacing of 0.05° based on site conditions. The figure shows a comparison of our model (*Mixed* model, on the left), the SHARE model (FSBG logic tree branch, in the middle) and the current Italian national seismic hazard map (MPS04, on the right). The same GMPEs (Akkar et al. 2013, Chiou et al., 2008, Faccioli et al., 2010 and Zhao et al., 2006 and Bindi et al. 2014), were used for all models to obtain and compare the maps.

Unknown
Formattato: Tipo di carattere:12 pt

Alessandro 28/8/y 15:00

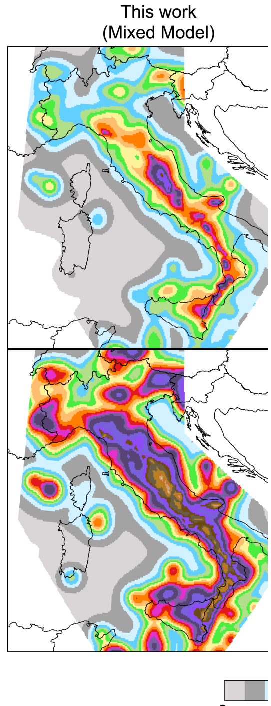

Eliminato:

Alessandro 28/8/y 15:02
Commenta [19]: After Main Comment number 2 and 3 and Detailed Comment L30 and L558-559 by RC1; and General Comment number 3 and and Section Specific Comment L63-68 by RC2.

ID	Fault Sources	L (km)	Dip (°)	Upper (km)	Lower (km)	SR_{min} (mm/yr)	SR_{max} (mm/yr)
1	Lunigiana	43.8	40	0	5	0.28	0.7
2	North Apuane Transfer	25.5	45	0	7	0.33	0.83
3	Garfagnana	26.9	30	0	4.5	0.35	0.57
4	Garfagnana Transfer	47.1	90	2	7	0.33	0.83
5	Mugello	21.0	40	0	7	0.33	0.83
6	Ronta	19.3	65	0	7	0.17	0.5
7	Poppi	17.1	40	0	4.5	0.33	0.83
8	Città di Castello	22.9	40	0	3	0.25	1.2
9	M.S.M. Tiberina	10.5	40	0	2.5	0.25	0.75
10	Gubbio	23.6	50	0	6	0.4	1.2
11	Colfiorito System	45.9	50	0	8	0.25	0.9
12	Umbra Valley	51.1	55	0	4.5	0.4	1.2
13	Vettore-Bove	35.4	50	0	15	0.2	1.05
14	Nottoria-Preci	29.0	50	0	12	0.2	1
15	Cascia-Cittareale	24.3	50	0	13.5	0.2	1
16	Leonessa	14.9	55	0	12	0.1	0.7
17	Rieti	17.6	50	0	10	0.25	0.6
18	Fucino	82.3	50	0	13	0.3	1.6
19	Sella di Corno	23.1	60	0	13	0.35	0.7
20	Pizzoli-Pettino	21.3	50	0	14	0.3	1
21	Montereale	15.1	50	0	14	0.25	0.9
22	Gorzano	28.1	50	0	15	0.2	1
23	Gran Sasso	28.4	50	0	15	0.35	1.2
24	Paganica	23.7	50	0	14	0.4	0.9
25	Middle Aternum Valley	29.1	50	0	14	0.15	0.45
26	Campo Felice-Ovindoli	26.2	50	0	13	0.2	1.6
27	Carsoli	20.5	50	0	11	0.35	0.6
28	Liri	42.5	50	0	11	0.3	1.26
29	Sora	20.4	50	0	11	0.15	0.45
30	Marsicano	20.0	50	0	13	0.25	1.2
31	Sulmona	22.6	50	0	15	0.6	1.35
32	Maiella	21.4	55	0	15	0.7	1.6
33	Aremogna C.Miglia	13.1	50	0	15	0.1	0.6
34	Barrea	17.1	55	0	13	0.2	1
35	Cassino	24.6	60	0	11	0.25	0.5
36	Ailano-Piedimonte	17.6	60	0	12	0.15	0.35
37	Matese	48.3	60	0	13	0.2	1.9
38	Bojano	35.5	55	0	13	0.2	0.9
39	Frosolone	36.1	70	11	25	0.35	0.93
40	Ripabottoni-San Severo	68.3	85	6	25	0.1	0.5
41	Mattinata	42.3	85	0	25	0.7	1
42	Castelluccio dei Sauri	93.2	90	11	22	0.1	0.5
43	Ariano Irpino	30.1	70	11	25	0.35	0.93
44	Tammaro	25.0	60	0	13	0.35	0.93
45	Benevento	25.0	55	0	10	0.35	0.93
46	Volturno	15.7	60	1	13	0.23	0.57
47	Avella	20.5	55	1	13	0.2	0.7
48	Ufita-Bisaccia	59.0	64	1.5	15	0.35	0.93
49	Melfi	17.2	80	12	22	0.1	0.5
50	Irpinia Antithetic	15.0	60	0	11	0.2	0.53

51	Irpinia	39.7	65	0	14	0.3	2.5
52	Volturara	23.7	60	1	13	0.2	0.35
53	Alburni	20.4	60	0	8	0.35	0.7
54	Caggiano-Diano Valley	46.0	60	0	12	0.35	1.15
55	Pergola-Maddalena	50.6	60	0	12	0.20	0.93
56	Agri	34.9	50	5	15	0.8	1.3
57	Potenza	17.8	90	15	21	0.1	0.5
58	Palagianello	73.3	90	13	22	0.1	0.5
59	Monte Alpi	10.9	60	0	13	0.35	0.9
60	Maratea	21.6	60	0	13	0.46	0.7
61	Mercure	25.8	60	0	13	0.2	0.6
62	Pollino	23.8	60	0	15	0.22	0.58
63	Castrovillari	10.3	60	0	15	0.2	1.15
64	Rossano	14.9	60	0	22	0.5	0.6
65	Crati West	49.7	45	0	15	0.84	1.4
66	Crati East	18.4	60	0	8	0.75	1.45
67	Lakes	43.6	60	0	22	0.75	1.45
68	Fuscalto	21.1	60	2	22	0.75	1.45
69	Piano Lago-Decollatura	25.0	60	1	15	0.23	0.57
70	Catanzaro North	29.5	80	3	20	0.75	1.45
71	Catanzaro South	21.3	80	3	20	0.75	1.45
72	Serre	31.6	60	0	15	0.7	1.15
73	Vibo	23.0	80	0	15	0.75	1.45
74	Sant'Eufemia Gulf	24.8	40	1	11	0.11	0.3
75	Capo Vaticano	13.7	60	0	8	0.75	1.45
76	Coccorino	13.3	70	3	11	0.75	1.45
77	Scilla	29.7	60	0	13	0.8	1.5
78	Sant'Eufemia	19.2	60	0	13	0.75	1.45
79	Cittanova-Armo	63.8	60	0	13	0.45	1.45
80	Reggio Calabria	27.2	60	0	13	0.7	2
81	Taormina	38.7	30	3	13	0.9	2.6
82	Acireale	39.4	60	0	15	1.15	2.3
83	Western Ionian	50.1	65	0	15	0.75	1.45
84	Eastern Ionian	39.3	65	0	15	0.75	1.45
85	Climiti	15.7	60	0	15	0.75	1.45
86	Avola	46.9	60	0	16	0.8	1.6

Table 1 Geometric Parameters of the Fault Sources. L, along-strike length; Dip, inclination angle of the fault plane; Upper and Lower, the thickness bounds of the local seismogenic layer; SRmin and SRmax, the slip rates assigned to the sources using the references available (see the supplemental files); and *ID*, the fault number identifier.

ID	Fault Sources	Historical Earthquakes yyyy/mm/dd	I_{Max}	I_0	M_w	sD	Instrumental Earthquakes yyyy/mm/dd	M_w
1	Lunigiana	1481/05/07	VIII	VIII	5.6	0.4		
		1834/02/14	IX	IX	6.0	0.1		
2	North Apuane Transfer	1837/04/11	X	IX	5.9	0.1		
3	Garfagnana	1740/03/06	VIII	VIII	5.6	0.2		
		1920/09/07	X	X	6.5	0.1		
4	Garfagnana Transfer							
5	Mugello	1542/06/13	IX	IX	6.0	0.2		
		1919/06/29	X	X	6.4	0.1		
6	Ronta							
7	Poppi							
8	Città di Castello	1269			5.7			
		1389/10/18	IX	IX	6	0.5		
		1458/04/26	VIII-IX	VIII-IX	5.8	0.5		
		1789/09/30	IX	IX	5.9	0.1		
9	M.S.M. Tiberina	1352/12/25	IX	IX	6.3	0.2		
		1917/04/26	IX-X	IX-X	6.0	0.1		
10	Gubbio						1984/04/29	5.6
11	Colfiorito System	1279/04/30	X	IX	6.2	0.2	1997/09/26	5.7
		1747/04/17	IX	IX	6.1	0.1	1997/09/26	6
		1751/07/27	X	X	6.4	0.1		
12	Umbra Valley	1277		VIII	5.6	0.5		
		1832/01/13	X	X	6.4	0.1		
		1854/02/12	VIII	VIII	5.6	0.3		
13	Vettore-Bove						2016/10/30	6.5
14	Nottoria-Preci	1328/12/01	X	X	6.5	0.3	1979/09/19	5.8
		1703/01/14	XI	XI	6.9	0.1		
		1719/06/27	VIII	VIII	5.6	0.3		
		1730/05/12	IX	IX	6.0	0.1		
		1859/08/22	VIII-IX	VIII-IX	5.7	0.3		
		1879/02/23	VIII	VIII	5.6	0.3		
15	Cascia-Cittareale	1599/11/06	IX	IX	6.1	0.2		
		1916/11/16	VIII	VIII	5.5	0.1		
16	Leonessa							
17	Rieti	1298/12/01	X	IX-X	6.3	0.5		
		1785/10/09	VIII-IX	VIII-IX	5.8	0.2		
18	Fucino	1349/09/09	IX	IX	6.3	0.1		
		1904/02/24	IX	VIII-IX	5.7	0.1		
		1915/01/13	XI	XI	7	0.1		
19	Sella di Corno							
20	Pizzoli-Pettino	1703/02/02	X	X	6.7	0.1		
21	Montereale							
22	Gorzano	1639/10/07	X	IX-X	6.2	0.2		
		1646/04/28	IX	IX	5.9	0.4		
23	Gran Sasso							
24	Paganica	1315/12/03	VIII	VIII	5.6	0.5	2009/06/04	6.3
		1461/11/27	X	X	6.5	0.5		
25	Middle Aternum Valley							
26	Campo Felice-Ovindoli							
27	Carsoli							
28	Liri							
29	Sora	1654/07/24	X	IX-X	6.3	0.2		
30	Marsicano							
31	Sulmona							
32	Maiella							
33	Aremogna C.Miglia							
34	Barrea						1984/05/07	5.9
35	Cassino							
36	Ailano-Piedimonte							
37	Matese	1349/09/09	X-XI	X	6.8	0.2		

Formattato ... [120]
Authors 28/8/y 12:12 Formattato ... [121]
Authors 28/8/y 12:12 Formattato ... [122]
Authors 28/8/y 12:12 Eliminato: Id
Authors 28/8/y 12:12 Formattato ... [123]
Authors 28/8/y 12:12 Formattato ... [124]
Authors 28/8/y 12:12 Formattato ... [125]
Authors 28/8/y 12:12 Formattato ... [126]
Authors 28/8/y 12:12 Formattato ... [127]
Authors 28/8/y 12:12 Formattato ... [128]
Authors 28/8/y 12:12 Formattato ... [129]
Authors 28/8/y 12:12 Formattato ... [130]
Authors 28/8/y 12:12 Formattato ... [131]
Authors 28/8/y 12:12 Formattato ... [132]
Authors 28/8/y 12:12 Formattato ... [133]
Authors 28/8/y 12:12 Formattato ... [134]
Authors 28/8/y 12:12 Formattato ... [135]
Authors 28/8/y 12:12 Formattato ... [136]
Authors 28/8/y 12:12 Formattato ... [137]
Authors 28/8/y 12:12 Formattato ... [138]
Authors 28/8/y 12:12 Formattato ... [139]
Authors 28/8/y 12:12 Formattato ... [140]
Authors 28/8/y 12:12 Formattato ... [141]
Authors 28/8/y 12:12 Eliminato: 15
Authors 28/8/y 12:12 Formattato ... [142]
Authors 28/8/y 12:12 Formattato ... [143]
Authors 28/8/y 12:12 Formattato ... [144]
Authors 28/8/y 12:12 Formattato ... [145]
Authors 28/8/y 12:12 Formattato ... [146]
Authors 28/8/y 12:12 Formattato ... [147]
Authors 28/8/y 12:12 Formattato ... [148]
Authors 28/8/y 12:12 Formattato ... [149]
Authors 28/8/y 12:12 Formattato ... [150]
Authors 28/8/y 12:12 Formattato ... [151]
Authors 28/8/y 12:12 Formattato ... [152]
Authors 28/8/y 12:12 Formattato ... [153]
Authors 28/8/y 12:12 Formattato ... [154]
Authors 28/8/y 12:12 Formattato ... [155]
Authors 28/8/y 12:12 Formattato ... [156]
Authors 28/8/y 12:12 Formattato ... [157]

38	Bojano	1805/07/26	X	X	6.7	0.1		
39	Frosolone	1456/12/05	XI	XI	7	0.1		
40	Ripabottoni-San Severo	1627/07/30	X	X	6.7	0.1	2002/10/31	5.7
		1647/05/05	VII-VIII	VII-VIII	5.7	0.4		
		1657/01/29	IX-X	VIII-IX	6.0	0.2		
41	Mattinata	1875/12/06	VIII	VIII	5.9	0.1		
		1889/12/08	VII	VII	5.5	0.1		
		1948/08/18	VII-VIII	VII-VIII	5.6	0.1		
42	Castelluccio dei Sauri	1361/07/17	X	IX	6	0.5		
		1560/05/11	VIII	VIII	5.7	0.5		
		1731/03/20	IX	IX	6.3	0.1		
43	Ariano Irpino	1456/12/05			6.9	0.1		
		1962/08/21	IX	IX	6.2	0.1		
44	Tammaro	1688/06/05	XI	XI	7	0.1		
45	Benevento							
46	Volturno							
47	Avella	1499/12/05	VIII	VIII	5.6	0.5		
48	Ufita-Bisaccia	1732/11/29	X-XI	X-XI	6.8	0.1		
		1930/07/23	X	X	6.7	0.1		
49	Melfi	1851/08/14	X	X	6.5	0.1		
50	Irpinia Antithetic							
51	Irpinia	1466/01/15	VIII-IX	VIII-IX	6.0	0.2	1980/11/23	6.8
		1692/03/04	VIII	VIII	5.9	0.4		
		1694/09/08	X	X	6.7	0.1		
		1853/04/09	IX	VIII	5.6	0.2		
52	Volturara							
53	Alburni							
54	Caggiano-Diano Valley	1561/07/31	IX-X	X	6.3	0.1		
55	Pergola-Maddalena	1857/12/16			6.5			
		1857/12/16			6.3			
56	Agri							
57	Potenza	1273/12/18	VIII-IX	VIII-IX	5.8	0.5	1990/05/05	5.8
58	Palagianello							
59	Monte Alpi							
60	Maratea							
61	Mercure	1708/01/26	VIII-IX	VIII	5.6	0.6	1998/09/09	5.5
62	Pollino							
63	Castrovillari							
64	Rossano	1836/04/25	X	IX	6.2	0.2		

65	Crati West	1184/05/24	IX	IX	6.8	0.3
		1870/10/04	X	IX-X	6.2	0.1
		1886/03/06	VII-VIII	VII-VIII	5.6	0.3
66	Crati East	1767/07/14	VIII-IX	VIII-IX	5.9	0.2
		1835/10/12	X	IX	5.9	0.3
67	Lakes	1638/06/08	X	X	6.8	0.1
68	Fuscalto	1832/03/08	X	X	6.6	0.1
69	Piano Lago-Decollatura					
70	Catanzaro North	1638/03/27			6.6	
71	Catanzaro South	1626/04/04	X	IX	6.1	0.4
72	Serre	1659/11/05	X	X	6.6	0.1
		1743/12/07	IX-X	VIII-IX	5.9	0.2
		1783/02/07	X-XI	X-XI	6.7	0.1
		1791/10/13	IX	IX	6.1	0.1
73	Vibo					
74	Sant'Eufemia Gulf	1905/09/08	X-XI	X-XI	7	0.1
75	Capo Vaticano					
76	Coccorino	1928/03/07	VIII	VII-VIII	5.9	0.1
77	Scilla					
78	Sant'Eufemia	1894/11/16	IX	IX	6.1	0.1
79	Cittanova-Armo	1509/02/25	IX	VIII	5.6	0.4
		1783/02/05	XI	XI	7.1	0.1
80	Reggio Calabria					
81	Taormina	1908/12/28	XI	XI	7.1	0.2
82	Acireale	1818/02/20	IX-X	IX-X	6.3	0.1
83	Western Ionian	1693/01/11	XI	XI	7.3	0.1
84	Eastern Ionian					
85	Climiti					
86	Avola					

Table 2 Earthquake-Source Association Adopted for Fault Sources. $I_{Max,}$ maximum intensity; I_0, epicentral intensity; M_w, moment magnitude; and sD, standard deviation of the moment magnitude. For references, see the supplemental files.